Supplement S1. Modeling System Design and Parameterization

The TOC and lists of figures and tables are hotlinked to their respective locations in the Supplement. For easiest navigation, open the bookmarks tab and expand the sections to locate any section or subsection. Then use the bookmarks to return to the TOC or go to any other section.

Table of Contents

List of Figures

List of Tables

Modeling System Design and Parameterization

The following presents a detailed summary of the core social and ecological submodels that run each annual time step in Envision, focusing on those that interact most directly with the wildfire model. Submodels are presented in the same order as in the manuscript. Social system submodels include human population growth (Section 1), landowner decision-making (Section 2), and landscape production feedbacks (Section 3). Ecological system submodels include climate-driven vegetation succession (Section 4), wildfire disturbances (Section 5) and finally the fire-decisions-succession execution sequence (Section 6). Although we refer to "Envision" throughout, we note that the specifics of our modeling system were developed for this particular project and are not necessarily represented in other applications of the Envision model.

1. Population Growth Submodel

The human population growth and land use allocation submodel spatially assigns new residents to the study area based on Oregon's statewide land use planning system. The system establishes and updates urban growth boundaries (UGBs) to constrain the spatial extent of urban and exurban development, and simultaneously protects productive rural land uses by establishing exclusive farm and forest use zoning. Agents can modify rural zoning when an IDU qualifies for a zoning change policy, creating opportunities for new rural housing by increasing density in existing rural residential zones or changing farm and forest zones into rural residential zones. The construction of new rural dwelling units, as well as UGB expansion, are driven jointly by study area population growth and the allocation of new housing to urban v. rural areas under different development scenarios. New dwelling units are assigned to rural and urban IDUs based on their available population capacity, which is determined by the difference between the IDU's current number of dwelling units and the maximum number allowed under it zoning. The simulated population growth rate was parameterized to achieve State of Oregon population growth projections for the study area for 2007-2056, while urban development was distributed based on the projected proportional allocation of population growth to each urban area [2].

2. Landowner Decision-making Submodel

2.1 Agent Decision-making Overview

Agents were assigned to IDUs to represent the diversity of landowners in the landscape, their values, and their spatial locations. Agent types, values and spatial distribution were determined using data from a mail survey of rural landowners in the southern Willamette Valley [3, 4]. Five types of agents were identified: rural residents, multipurpose smallholders, farmers, foresters, and forested estates. Each agent type was parameterized with a suite of six values derived from the survey that respectively represent their differing propensities to manage the land to earn a living, avoid wildfire risk, benefit the environment, and respond to climate change, as well as their responsiveness to financial incentives, and the importance of property rights to their decisions. Values were assigned to individual agents based on statistical profiles of the mean and variability of values for each agent type to mimic the nuances of individual landowners and their values in the actual landscape. Similarly, agent types were assigned

probabilistically to IDUs based on statistical profiles of the land characteristics (e.g., land cover, tax lot size, etc.) of each agent type to mimic the nuances of landowner distribution in the actual landscape.

Individual agents seek to manage an IDU under their control in ways that are consistent with their values and in response to landscape scarcities through the adoption of policies, which include all possible actions available to them in relation to the IDU under their control. They can change the current state of their IDU, and in doing so, may alter successional trajectories or future development locations. When an agent changes zoning on a farm or forest parcel to allow new development, the agent type can change to a rural resident or multipurpose smallholder, affecting future management decisions. Agents can modify vegetation through short-term actions such as timber harvest, or longer-term management such as ecological restoration and fuels reduction treatments. Agent's choices about how to manage their land, when to do so, and how long to continue management, affect wildfire behavior through effects on vegetation and fuels.

Actions are implemented through the adoption of Envision *policies*, which represent private and public priorities supporting permissible land management actions that are consistent with scenario assumptions. Policies include fuels treatments, ecological restoration, agricultural and timber management, and rural housing development. Each policy is ranked on six dimensions of survey-calibrated agent values that affect the likelihood of policy adoption by different agent types and individual agents [3]. Agents choose actions that best align with their values, and in response to landscape-level productions and scarcities.

2.1.1 Submodel Design

When an agent makes a decision to act, they assess all policies available to them based its alignment with four factors: the agent's self-interests, the degree to which the policy serves to provide valued landscape productions and/or reduce scarcities (altruism), the degree to which it satisfies "global" policy preferences that are independent of agent values, and the degree to which the policy is assessed to have utility. For each policy the "distance" between its intended outcome and the factor in question is calculated, thus specifying four distance vectors. The distance scores are summed based on the weights assigned to each factor for that agent. The agent then selects the policy with the minimum total score (Figure S1.1). Although an agent's values remain constant over the course of a run, the distance between their values and specific policies is sensitive to landscape feedbacks through production and scarcity metrics.

Envision policy development is central to creating the raw materials of agent decision-making through which scenario assumptions and contrasts can be explored and tested. We used a combination of landowner survey results and other data developed specifically for this project, as well as available local and regional empirical data, and stakeholder guidance to develop and parameterize the suite of policies used in simulations. Policies can be targeted toward specific agent types, or have outcomes that vary by agent type, for example the maximum size of a restoration treatment or timber harvest. The areas that qualify for a policy can be targeted and constrained using any IDU attributes, including biological or physical attributes such as current or historical vegetation type, slope and aspect; cultural attributes such as taxlot boundaries, mapped zones (e.g., WUI type, conservation priority zones) or population density; distances from features such as roads or houses; locations with specified amounts of selected habitat types

within the surrounding area; timers that track past events (e.g., time in management, time since last disturbance); and so forth. Policies can be targeted to spatial extents that align with specific sociocultural intentions. For example, to protect individual homes, fuels reduction treatments could be assigned to single IDUs containing a rural home. On the other hand, to reduce fire spread rates, fuels treatments were applied to larger areas but constrained to a single taxlot parcel unless the policy was intended to represent a collaborative project among landowners.

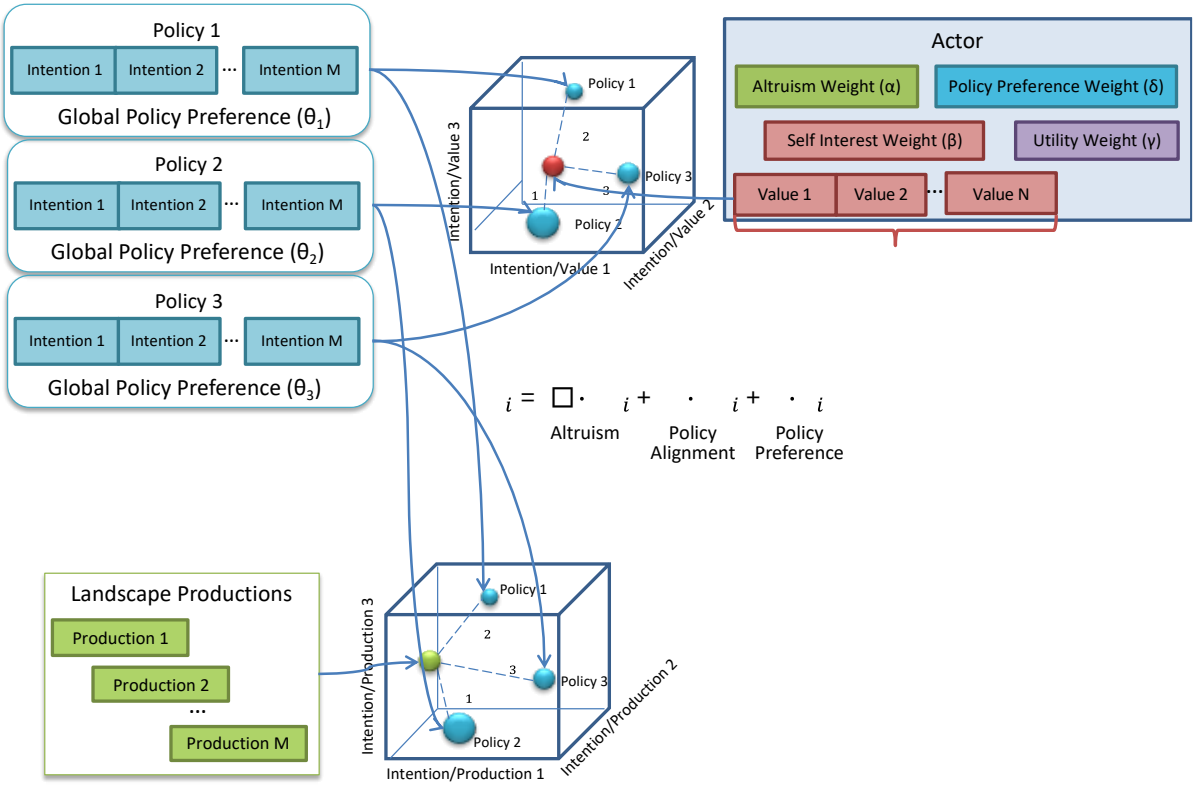

Figure S1.1. Agent decision-making algorithm. When making a decision, agents select the policy with the minimum combined score P_i, a multicriteria weighting based on altruism, agent value alignment, utility, and global preferences. The *altruism* score measures alignment between policy intentions and landscape production scarcities. The *self-interest* score measures alignment between policy intentions and agent values. *Global policy preferences* measure overall, agent-independent policy preferences.

2.1.2 Submodel Parameterization

We employed a number of mechanisms to make agent decisions conform to patterns observed in actual landscapes. For example, we assumed that, on average, individual agents would not implement new actions on their IDU more frequently than once every five years on the assumption that landowners don't make major changes every year. Further, some actions were linked to other Envision submodels to more closely mimic how they would actually occur. For example, the need for new rural development required changes in land use zoning when the existing capacity for new rural homes was insufficient to meet scenario-specific population growth assumptions. Thus, rural agents frequently had to first obtain a zoning change to build new homes in lands zoned for farming or forestry. Urban growth boundaries (UGB) were

updated every 10 years to mimic the periodicity of implementing Oregon's land use policies for urban expansion into rural areas, while WUI zone maps were updated at the same time.

2.1.2.1 Assigning agent decision rates

Application rates for each policy were calibrated using landowner survey responses [3, 4] or other empirical data. Where survey results revealed differences in decision propensities by agent type (rural residents, multipurpose smallholders, farmers, foresters, and forested estate owners), these were incorporated in separate policies for each agent type. For example, implementation of defensible space practices around rural homes was parameterized for each of the five agent types, and could change over time in response to wildfire risk. Similarly, the rates of pasture management (grazed or ungrazed, which affected fuel loadings) were parameterized by agent type. Timber harvest rates were calibrated using aerial photo analysis of the study area over the prior 10 years, and rates assumed to remain constant over the course of the simulation, except as altered by landscape feedbacks to agent values, because we did not attempt to simulate the market forces that drive harvest rates. High-quality restoration was emphasized for projects implemented with public funds, whereas lower-cost structural restorations were emphasized when costs were paid by private landowners. In some cases, policy application rates were modified for different scenarios to align with stakeholder-informed assumptions about key scenario contrasts, such as landowners' overall willingness to implement fuels treatments versus restoration.

2.1.2.2 Agent change

As noted previously, agent types and their spatial distribution were assigned based on landowner surveys. Both initial agent assignment and any subsequent changes were based on factors such as the IDU's size and landscape context. The initial agent assigned to an IDU was assumed to continue occupancy throughout the simulation run except when development was expected to change the agent type. For example, when IDUs under the control of farmers or foresters were rezoned to allow new rural residential housing, they became eligible for development. Subsequently, if a new rural residence was assigned to the IDU in response to population growth, either a rural residential agent or a multi-purpose smallholder agent was probabilistically assigned to the IDU to represent the change of land ownership. Furthermore, when the housing density around an IDU increased beyond a certain threshold, it was assumed that large-scale farming and forestry were no longer viable and remaining farmers and foresters were converted to rural residents or multipurpose smallholders. Because each individual agent and agent type had key differences in decision-making propensities for vegetation management and defensible space practices, changing an agent changed subsequent land management, as well as responses to landscape productions and scarcities.

2.2 Land Management Actions Overview

Vegetation management goals, treatment types, and BMPs were developed with advisory teams of regional experts and practitioners [5, 6]. Treatment effects were parameterized using the same regional tree lists as the successional model. The process generated six base management treatments: density thinning with surface fuels reduction, oak-pine savanna restoration, oak-pine woodland restoration, prairie restoration, silvicultural thinning, and commercial timber harvest,

and included two levels of restoration quality (Table S1.1). Density thinning was specified with fire hazard reduction as its sole goal. Savanna restoration was intended primarily for biodiversity conservation and secondarily for fire hazard reduction. Woodland restoration balanced conservation benefits with fire hazard reduction. Silvicultural thinning and timber harvest followed local practices and were calibrated to recent harvest rates. So long as an agent sustains active management, succession (Sect. 4) follows a constrained trajectory consistent with management goals and the BMPs applied. If an agent ceases management, treatment effects degrade on a specified timeline, until the IDU returns to an unmanaged state and successional trajectory.

Like other agent actions, management treatments are implemented through policies. Each treatment type is oriented toward specific vegetation types and locations to align with policy goals and agent values. For instance, fuels treatments targeted to high-hazard vegetation types, proximity to roads, parcels with residences, and areas with denser housing, while ecological restoration may be targeted to priority conservation areas based on regional maps, and areas with minimum thresholds of restorable habitat nearby. Vegetation best management practices (BMPs) were assigned to each combination of treatment type and vegetation-state to achieve intended outcomes. BMPs defined the specific actions agents took to achieve their goals. For example, two levels of ground-layer quality were defined for savanna and woodland restoration depending on whether the goal was primarily to restore tree canopy structure or to additionally create a high-quality native ground layer [6]. The specific outcomes of a treatment to a given IDU depended on the treatment type, the IDU's pretreatment state, and the specific BMPs applied. For example, an agent could apply oak woodland restoration to fir-oak forest, closed oak woodland or other forest types that qualified under the criteria specified in Envision policies. Survey results and stakeholder guidance were used to provide varied and nuanced ways for agents to respond to wildfire risk and habitat scarcity.

BMPs determined not only treatment effects on vegetation and fuels, but also the cost [6]. Treatment costs sometimes were offset by income from merchantable trees for lumber or woodchips. The board feet of lumber or chip volume, obtained from quantitative simulations, varied dramatically by vegetation state and treatment type, leading to large differences in net cost even for the same treatment type. In general, density thinning were least expensive, followed by structural and high-quality restorations, respectively. Any subsequent retreatment to prevent fuels regrowth required fewer and different BMPs but produced no offsetting income because any merchantable trees had been previously removed. Structural restorations were least expensive to maintain, high-quality woodland and density thinning nearly equal, and high-quality savanna the most expensive.

Supplement S1 *from* Exploring and testing wildfire risk decision-making in the face of deep uncertainty

Table S1.1. Management changes vegetation and fuels based on objectives and best management practices (BMPs). All treatments requiring thinning were simulated in FVS based on removal of smaller trees and/or retention of preferred species. Effects on fire depend on the pretreatment state and structural variant; typical effects are shown. See [6] for BMPs and detailed species and structural targets used to implement treatments. Prairie treatments match the ground layer goals and effects of structural and high-quality savanna restoration but with 0-5% tree canopy.

Treatment	**Management Goals**	**Expected Fire Effects**	**Example**
Density thinning w/ surface fuels reduction	Discontinuous tree canopy (≤ 40% cover; ~10' spacing between tree crowns); Reduction of surface and ladder fuels; Control of resprouting trees and shrubs	Reduced flame length, rate of spread (ROS) and crown fire potential	
Structural savanna restoration	Oak-pine-fire savanna (6-25% canopy cover); Reduced ladder fuels and shrub cover; Control of priority invasive species and resprouting trees and shrubs; Seed as needed with native bunchgrasses to create continuous herbaceous ground layer; Structural prairie identical except 1-5% canopy cover	Flame length +/-; ROS high in peak-fire season, low in off-season; Reduced crown fire potential	
High-quality savanna restoration	Savanna canopy as above; Intensive BMPs to create continuous herbaceous ground layer dominated by diverse native bunchgrasses and forbs w/low shrub cover; High-quality prairie identical except 1-5% canopy cover	Reduced flame length, ROS and crown-fire potential compared to structural savanna	

Treatment	**Management Goals**	**Expected Fire Effects**	**Example**
Structural woodland restoration	Open oak-pine woodland with discontinuous tree canopy (26-40% cover); Reduced ladder fuels and moderate shrub cover; Same ground layer BMPs as structural savanna but semi-continuous herbaceous ground layer (due to canopy shading) and higher shrub cover	Generally reduced flame length, ROS, and crown fire potential; ROS higher in peak-fire season and lower in off-season under identical ERCs; Lower flame length and ROS than structural savanna	
High-quality woodland restoration	Woodland canopy and shrub layer as above; BMPs to create semi-continuous herbaceous ground layer dominated by diverse native bunchgrasses and forbs	Reduced flame length, ROS and crown fire potential compared to structural woodland	
Silvicultural thinning	Pre-commercial thinning prior to timber harvest	Reduced potential for crown fire	
Timber harvest	Harvest of merchantable trees via clearcutting followed by replanting for future harvest	Depends on pretreatment states; Clearcuts develop dense herbaceous and shrub fuels	

The wildfire implications of applying a specified treatment type and associated BMPs varied substantially depending on the extant state. In general, simulated thinnings using regional tree lists (including restoration) reduced canopy cover and canopy bulk density, and increased canopy base height. As a result, thinning treatments tended to reduced flame lengths and crown fire potential but effects on fire spread rates depended on surface fuels. Our stakeholder advisory team noted, however, that one consequence of opening the tree canopy in the Willamette Valley's mild, wet winters is to increase herbaceous fuels production, which can slow fire spread rates and reduce flame lengths during the off-peak season when they largely remain green and increase spread rate and flame lengths during peak fire season when they are senesced. To this end, dynamic fuel models (Scott & Burgan 2005) were used to mimic seasonal dynamics of herbaceous plant senescence with summer drought, and green-up with fall rains. (Sect. 5.2.1.4).

2.2.1 Submodel Design

Land management policies can be written and implemented to support nuanced agent actions in the simulated landscape. Policies employ a grammar that can incorporate any set of IDU attributes to specify the range of site conditions under which a policy can be applied, the types of agent that may apply it, the likelihood it will be applied, when the policy can be applied, and how long the treatment remains in effect. When agents choose to act, they select from among the policies available for their IDU based on their values and goals, including those affected by dynamic landscape feedbacks from wildfire risk and conservation scarcity, as described above.

Most unmanaged successional vegetation states (Sect. 4) have a managed counterpart in terms of cover type and dominant tree diameter that follows a more constrained successional trajectory. For example, an unmanaged oak savanna may transition over time into a Douglas-fir forest. However, under oak savanna restoration, trees can grow larger but vegetation remains oak savanna. The restriction on cover type change was not applied to thin-from-below management, which was presumed to retain larger trees regardless of species and to allow dominant species to change as trees grew at different rates.

FVS thinning simulations were conducted for each treatment type on the full set of vegetation states, and associated replicate tree lists, that qualified for that treatment type. Both the outcome state, and the board feet of timber and chip volume removed by thinning, were recorded. Differences in the pretreatment state could lead to different post-treatment vegetation and fuels from the same management treatment application. Similarly, within a single pretreatment state, the presence of structural variants with trees larger than the QMD could lead to different outcomes for the same management treatment (Sect. 4.1). Following initial treatment, probabilities of successional change under each management type were projected using FVS [6] with similar protocols to those used to derive successional probabilities for unmanaged vegetation.

Management constraints on succession remain in place for a time period following treatment that depends on the treatment type applied. For example, more extensive modifications of surface fuels were assumed to last longer (e.g., the effects of converting a shrub understory to a grassland lasts longer than simply cutting back shrubs). Should an agent cease management, the IDU returned over time to an unmanaged vegetation state and fuels of the same dominant tree species and diameter class as the current managed counterpart. The time thresholds for each

treatment type varied depending on the expected length of BMP effects, rates of fuels accumulation, and vegetation change in the absence of further management. Default timelines are provided but can be modified by the user (Sect. 6).

Each managed vegetation state included up to 5 surface fuels variants that depended on treatment type and time since cessation of management (structural or high-quality restoration, thin-from-below, degraded restoration and degraded thin-from below). The only difference between structural and high-quality restoration of the same dominant species and QMD was the surface fuel model. Finally, we assumed that fuels on IDUs in unmanaged successional states would increase over time in the absence of disturbance (management or fire). Because both restoration and density thinning removed smaller trees, it was assumed that no further "thinning from below" would occur after a fire in a previously treated IDU. Instead, mixed-severity fires in managed stands could change cover types due to reduced canopy cover or mortality of less fire-resistant species but caused no further changes to the dominant size class.

With the exception of a policy targeting fuels treatments to single IDUs with houses, all fuels and restoration treatments were applied to contiguous blocks of qualifying IDUs up to a maximum size recommended by our stakeholder advisory team, which could vary by agent type and treatment type. Over time, such individual projects could aggregate into larger blocks. This prevented fragmentation of managed vegetation due to the fine-grained architecture of IDUs, which was based on intersecting taxlot parcels with soils polygons.

2.2.2 Submodel Parameterization

Based on landowner survey results and stakeholder guidance, we implemented a total of 59 policies to simulate different forms of fuels treatments, ecological restoration, timber harvest, commercial thinning, pasture management, alteration of agricultural land uses, or implementation defensible space practices around rural residences. Some policies were broken down by agent type to implement different adoption rates (e.g. defensible space) or maximum areas (e.g. restoration projects). Fuels treatments and restoration received the most detailed attention, including how publicly funded fuels treatments were differentially targeted toward the WUI v. non-WUI, to areas of greater risk such as around homes or zones of higher ignition probability such as along roads, and to vegetation types with different levels of fire hazard. Similarly, conservation-based restoration policies supported with public funds were targeted toward areas of highest conservation priority based on regional assessments, as well as areas with higher levels of restored or restorable habitat nearby. Landowner-funded policy adoption rates were based on survey results, sometimes by agent type, without regard to their public or landscape-scale benefits.

Density thinning was designed to follow common fire hazard reduction approaches. Thin-from-below procedures were applied in FVS to create a discontinuous canopy cover and raise canopy base height by removing smaller trees, as well as to reduce surface and ladder fuels. Savanna and woodland treatments targeted the creation of discontinuous canopies of fire-adapted oaks and pines with grassland understories. Woodland restoration assumed higher shrub cover and lower overall herbaceous fuel loads than savanna due to the increased canopy cover. Importantly for fire, the greater canopy cover of a mature woodland better retained humidity in surface fuels and reduced wind speeds than in a savanna.

As noted previously, differences in the pretreatment vegetation state or its variants can lead to different outcomes for the same management treatment depending on the species, sizes and densities of pretreatment trees. For example, an oak-pine woodland treatment could result in a savanna if there were not enough oak and pines to maintain the targeted 40% canopy cover after thinning other conifers. Under continued woodland management, however, such a stand could attain woodland structure and canopy cover as trees grew and new trees established. In the case of "extreme makeover" restoration, which assumed that a former grassland that had completely succeeded to conifer forest was restored to oak savanna or woodland, planting oaks was included as a BMP and these young oaks were projected to grow and mature over time.

The BMPs applied for structural restorations were designed to reduce shrub cover, ladder fuels and invasive introduced species and, when needed, to include seeding with a simple mix of native bunchgrasses. High-quality restorations assumed the application of more extensive and expensive BMPs to replace introduced cool season grasses with a diverse mix of native bunchgrasses and forbs. All prairie restorations were assumed to be high quality. Surface fuels variants were used to designate ground-layer differences in otherwise identical cover types due to management or its absence (e.g., high-quality versus structural restoration, or the degradation of treatment effects following cessation of management). Biomass data from two local grassland studies [7, 8] were used to calibrate herbaceous fuel loadings for restored and unmanaged prairies and savannas. Given the sensitivity of fire simulations to grassland fires, and the very different fuel loadings of grazed and ungrazed pastures, we assigned different fuel models to grazed and ungrazed pastures, and assigned pasture management by agent type based on the landowner survey.

Applying savanna or prairie restoration treatments to woodlands or forests led to the greatest increases in herbaceous fuels of all treatment applications. By creating sparse canopy cover, they also increased wind speed near the ground in FlamMap. The higher canopy cover of woodland restoration constrained herbaceous fuels and wind speed compared to savanna and prairie but was associated with higher herbaceous fuel loads than density thinning because the latter has higher canopy cover, leading to less grass and more leaf litter in the associated surface fuels. For structural restorations, management of thatch and invasive grasses was assumed to reduce herbaceous fuels over unmanaged grasslands, including unmanaged prairies and ungrazed pastures. High-quality restorations, by replacing introduced cool season grasses (which create a tall, continuous fuel bed) with native bunchgrasses and forbs (with a more heterogeneous, discontinuous fuel bed) reduced fuel continuity, flame length and rates of spread relative to unmanaged states and structural restorations of equivalent canopy structure. See Sect. 5.2.1.4 for a description of how this led to the use of dynamic fuels models to simulate the transition from live herbaceous fuels during the rainy season to dead herbaceous fuels in the summer drought and back to live herbaceous fuels with the initiation of fall rains and subsequent green-up. The use of dynamic fuel models reduced flame lengths and fire spread rates when herbaceous fuels were alive but increased them after senescence during the summer drought.

3. Landscape Production Submodels

3.1 Overview

Landscape production submodels provide the mechanism for feedbacks from landscape change to influence agent decision-making. They rely on metrics of landscape change that are selected to represent the interactive and cumulative effects of all simulated SES landscape change drivers and processes – climate change, population growth, development, succession, vegetation management and wildfire – on valued economic productions and ecosystem services. To this end, two landscape production and scarcity metrics were calculated annually at the study area scale: a wildfire risk metric based on residences recently threatened by wildfire, and a conservation metric based on managed area of regionally imperiled prairie and oak grasslands. The associated feedback algorithms to the agent-decision submodel were parameterized based on the expected sensitivity of policy makers and landowners to residential risk from wildfire, and to the attainment of regional conservation targets, respectively. The wildfire metric (based on the five-year running average of the number of residences threatened by wildfire) is thus linked to the agents' averseness to fire risk. The conversation metric for prairie-oak grasslands (based on the degree to which conservation goals for recovery of imperiled grasslands have been achieved) is linked to agents' valuation of environmental conservation.

Both metrics influence the decisions of individual agents by differentially influencing policy adoption rates for each agent type based on landowner survey responses. To do this, each metric served as one of the six agent value parameters, allowing each agents' responsiveness to policies targeted to mitigation wildfire risk or expanding oak-prairie restoration to change over time. Each agent type has a distribution of sensitivities to each of the six values, and each individual agent is assigned its own value ratings accordingly. This creates an array of sensitivities to each metric within each agent type. Simultaneously, each policy (e.g., possible agent action) is rated in terms of its relationship to each of the six agent values. The decision model algorithms guide agents to take actions that are consistent with their values. Production and scarcity metrics thus influence the degree to which a given policy may serve the agent's values in relation to the current state of the landscape. In this way, the metrics mediate individualistic goal-seeking behavior toward coordinated actions intended to minimize scarcities. As described next, the wildfire risk metric was also used to regulate the flow of public incentives funding for fuels treatments and ecological restoration, thus representing a top-down form of influence on landowner behaviors by policy makers.

3.2 Wildfire Risk Metric

Of particular importance vis-à-vis simulated wildfire risk mitigation is a feedback based on the number of homes threatened by recent wildfires. As described above, greater numbers of threatened residences increase the likelihood that agents who are responsive to wildfire risk will implement actions to reduce it. Second, greater numbers of threatened residences increase the proportion of public funds allocated to fuels reduction treatments versus ecological restoration. Each of these two submodels applied the risk metric using a specific algorithm calibrated to produce the desired feedbacks. The former is described in this section and the latter in the public incentives section.

Residences in an IDU that burned in a wildfire were considered threatened based on a) whether the agent had implemented defensible space practices around their home and b) fire severity combined with the amount and structure of hazardous fuels. Defensible space protected residences only when they were exposed to low-severity fire or in vegetation types with very sparse tree canopy, like savanna. In forests and woodlands, with more continuous canopies and ladder fuels, the potential for active crown fire or torching (i.e., mixed- or high-severity fire with ember showers) meant that a home was considered threatened even with defensible space practices. The specific rules implemented for a residence in an IDU that burned were as follows:

a) In the absence of defensible space practices, fire threatens a residence in an IDU that burns regardless of fire severity.

b) Defensible space practices protect a residence exposed to a low-severity fire, defined as one with insufficient tree mortality to change the vegetation state.

c) Defensible space practices do not protect residences in an IDU that experiences a mixed-severity or high-severity fire (that is, with sufficient tree mortality to change the vegetation class) except in savannas, with their widely spaced trees and herbaceous fuels, and in density-thinned forest and woodlands dominated by sapling-sized trees and with reduced surface and ladder fuels. These vegetation classes can be identified using Supplement S2: Sect. 2.

The wildfire risk metric converted annual counts of threatened residences into a five-year running average of threatened residences. As described next, this metric was applied using two different algorithms to modify agents' policy adoption likelihood, and the proportional allocation of public incentive funds (Sect. 3.3), respectively.

Envision production and scarcity policy algorithms are set on a scale of -3 to +3 where 0 means that agents implement policies without additional landscape feedbacks to modify policy adoption rates. When risk from wildfire is low (values less than 0), agents experience less impetus to adopt policies designed to reduce wildfire risk. As wildfire risk increases above the no-effect threshold (values greater than 0), agents become more likely to adopt policies intended to reduced wildfire risk. The algorithm was calibrated a minimum value of -2.4 when no residence burned over a 5-year period. Because almost no study-area residences had been threatened from wildfire in recent decades prior to 2007, the scale quickly jumped to 1 when an average of just one structure was threatened every five years and to 2 when an average of 10 structures were threatened per year on the expectation that residents would respond strongly to even a few threatened residences (Figure S1.2).

The wildfire risk response algorithm for agent policy adoption uses a logarithmic function of the 5-year average number of threatened residences (x):

$$y = a*(\log(x+b)^{(x+c)})/(x+b) \text{ with values of } a = 1.5,\ b = 0.584 \text{ and } c = 4$$

where *a* is a scale parameter that adjusts the limit of y, *b* is a shape parameter that influences the shape of the curve around its inflection point, and *c* is a second shape parameter designed to have a larger impact when *x* is small than when *x* is large. A

final modification limited the minimum to -3 and maximum to +3 should the wildfire metric inputs cause the formula to exceed these values.

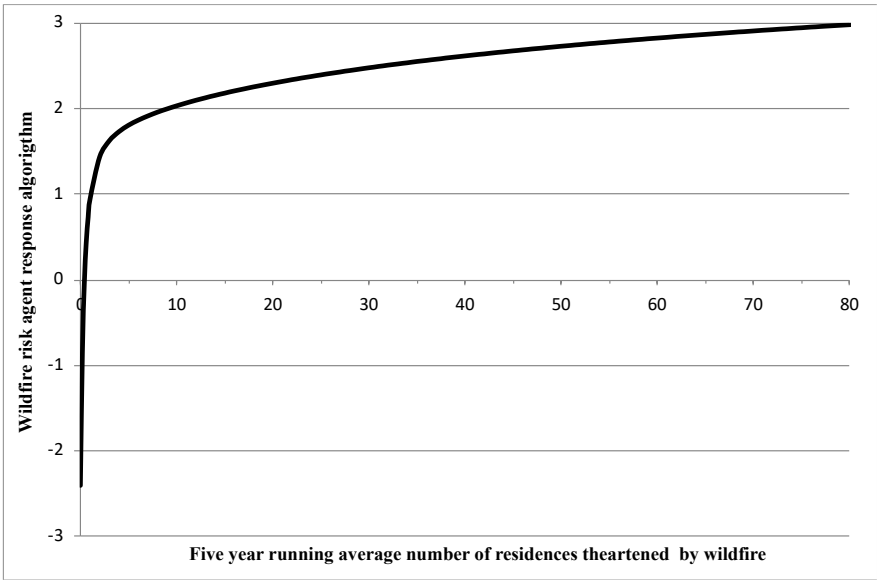

Figure S1.2. Wildfire risk agent response algorithm. The response algorithm varies from -3 to +3 and represents a measure against which the societal goal of mitigating wildfire risk is evaluated. Values > 0 increase agent propensities to restore native grasslands. Values < 0 decrease agent propensities to reduce wildfire risk, while values >0 increase their propensities.

3.3 Public Incentives Budget System

Landowner surveys revealed that people's willingness to implement management treatments depended largely on whether they received financial support [3]. Fuels treatment and restoration policies were therefore differentiated as those that assumed agents paid all associated costs versus those supported by public funding; adoption rates were parametrized based on survey results. A budget system tracked expenditures for publicly funded projects so that such treatments could be capped to scenario-defined annual public incentives budgets.

In addition to capping public expenditures to support these two societally valued services, the budget system applied user-specified assumptions about policy-makers sensitivity to supporting wildfire risk reduction versus conservation priorities based on recent wildfire risk to homes. To this end, an algorithm based on the wildfire risk metric's five-year running average of threatened residences determined each year's allocation of public incentives funds to support either fuels treatments or ecological restoration. Greater numbers of recently threatened residences directed more public funding to fuels treatments (Figure S1.3).

Like other landscape productions and scarcities, the algorithm for the threatened residence metric, and how it affects the use of public funds, is controlled by the user and can be altered as desired. In our use, publicly funded projects had more stringent requirements than landowner-funded projects. For example, publicly funded fuels treatments were targeted to high-risk WUI, while ecological restoration was targeted to conservation priority zones and/or locations with large surrounding areas of restorable habitat.

A key scenario contrast was the designation of which management actions could serve as fuels treatments versus ecological restoration. In Hazard Reduction scenarios, only density thinning could be funded as a fuels treatment, whereas in Restoration scenarios, oak and pine woodland restoration could be paid for under either budget depending on whether it was targeted toward areas of high conservation priority or high fire risk. Oak and pine woodland restoration were chosen as the only ecological restoration treatment that could also be supported by public funds as a fuels treatment because it targeted separation between tree canopies which maintaining enough canopy cover to retain humidity in surface fuels and reduce wind speeds.

Furthermore, restoration scenarios included a publicly funded policy for "extreme makeover" of restoring small areas of former grassland that had converted conifer forest with no remaining oak. Policies variously supported planted oak savanna (restoration budget) or planted oak woodland (fuels treatment budget). Extreme makeover treatments were only conducted on sites adjacent to substantial areas of restored oak habitats as a means to create larger contiguous blocks of restored oak with little added expense since the qualifying forest types typically contained enough merchantable conifers to offset treatment costs. Application rates were relatively low since our surveys showed few current landowners were interested in conducting such projects. Extreme makeover was only allowed in Restoration scenarios, which assumed greater overall willingness to implement restoration. Because areas that had converted to completely conifer forest tended to have productive soils, this policy had the added benefits of recovering oak habitats in areas that would quickly grow large oaks, while restoring native grasslands across their full historical range of variation or HRV (Wiens et al. 2012).

Costs were assessed on a per hectare basis for each combination of treatment-type and extant vegetation-state. The net cost was the sum of the costs of each best management practice (BMP) needed to achieve the desired outcome minus any profits from merchantable trees removed by thinning. Different BMPs could be required to achieve the same desired management outcome depending on pretreatment vegetation and fuels. The budget system assumed an average timber board feet and woodchip volume for each vegetation state and management treatment combination (Sect. 2.2.1), and used the average prices from recent high and low market prices [6]. Once a stand had been thinned, it was assumed that no further timber or chips would be produced from subsequent retreatments.

BMPs were prescribed for 10 years post-treatment to derive associated costs. The cost for an entire project was summed across all IDUs included in the treatment block. Each time an incentivized policy was applied, funds were deducted from the appropriate budget. Treatment applications that returned a profit were "zeroed out" so that no funds were deducted from the budget. Once the annual budget for fuels treatments or restoration was spent, no further incentivized policies of that type could be adopted that year. Agents could, however, continue to implement treatments using policies that assumed the agent paid all costs.

Proportional Allocation of Fire Hazard and Restoration Budgets

The % of budget allocated to Fire Hazard is based on a basic decay function where the parameter m sets the maximum amount of budget to fire hazard, x sets the minimum amount of budget to fire hazard, and h sets the rate at which the function approaches the maximum. The function is based on a 5-year running average of the number of threatened residences (TRs). The current function is set so that the % of the total budget allocated to fire hazard reaches a maximum of 88% when ~5 houses/year have been threatened in the last five years (a total of 25 houses over 5 years). The % Restoration is set to 1 minus the % Fire Hazard. The example Budget Allocation graphs for scenarios LCC, HCM, and HDC were created by applying the proportional allocation function to the tally of threatened residences in each year from one run of each scenario.

Change the parameters in the yellow box to see how they change the allocation of incentivized funds to restoration (green) v. fire hazard (orange).

m controls the maximum percent that can be allocated to fire hazard and thus the minimum that can be applied to restoration.

x controls the minimum that can be applied to fire hazard & thus the maximum that can be applied to restoration (i.e. the percent when TRs = 0). However it interacts with m, so you may have to change m when you change x.

h controls the shape of the curve between the extremes. Increasing h decreases budget allocation sensitivity to threatened residences (i.e. it "pushes" the curve to the right). Decreasing h increases sensitivity.

Note: if you change a parameter and the formula "blows up" try a smaller change

Parameters Used		
m	**x**	**h**
0.6	0.4	1

5 yr avg. TRs	% Fire Hazard	% Rest-oration
0	40%	60%
1	41%	59%
2	43%	57%
3	48%	52%
4	57%	43%
5	69%	31%
6	78%	22%
7	84%	16%
8	86%	14%
9	87%	13%
10	88%	12%
11	88%	12%
12	88%	12%
13	88%	12%
14	88%	12%
15	88%	12%
16	88%	12%
17	88%	12%
18	88%	12%
19	88%	12%
20	88%	12%

The curves of the example runs will change when you alter the response curve parameters.

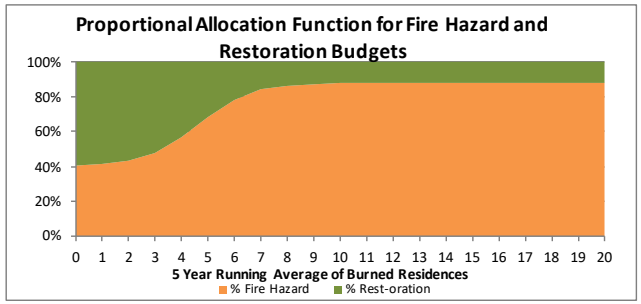

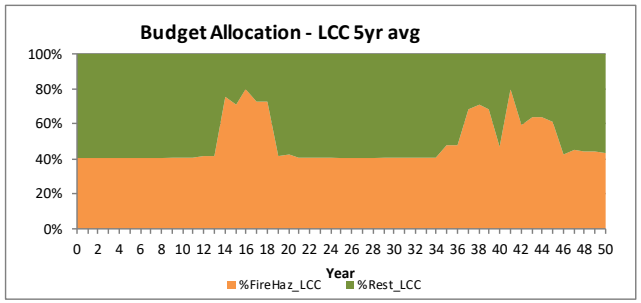

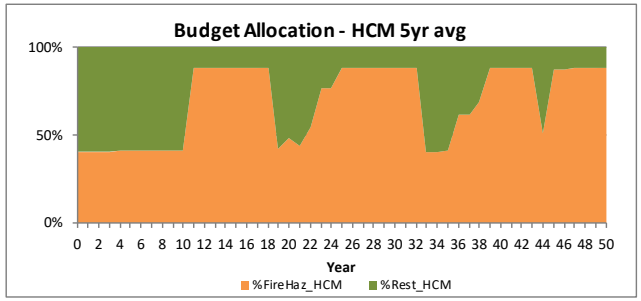

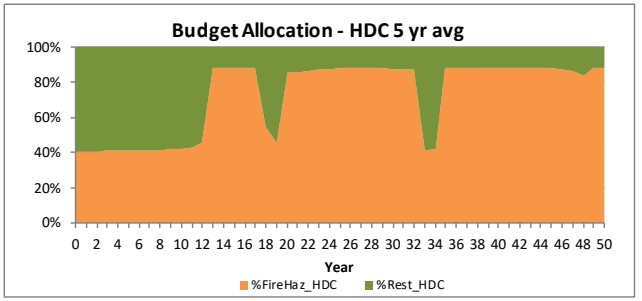

Figure S1.3. User-controlled proportional allocation formula for public incentives funding to fuels treatments versus ecological restoration.

3.4 Conservation Metric

The conservation scarcity model provides feedback to agent propensities to restore statewide conservation strategy habitats [9] for Willamette Valley prairie and oak grasslands. The metric was based on a general target used by The Nature Conservancy for recovering 30% of the pre-Euro-American settlement area of Willamette Valley ecosystems prioritized for conservation. Based on maps of historical vegetation created from 1851 General Land Office Survey maps [10], native grasslands, primarily oak savanna, upland prairie, and wetland prairie covered 57% of the study area (44,505 out of 78,039 ha). We did not include historical oak woodland in our calculations because it was likely dominated by a dense shrubby understory with few grasses and forbs, even though it may have had similar canopy cover to oak savanna. Furthermore, there is no current analog for this historical oak woodland since most contemporary oak woodland has a closed tree canopy.

The ground layer of historical grasslands was dominated by diverse mixtures of native bunchgrasses and forbs. The savanna tree layer was typically dominated by Oregon white-oak (*Quercus garryana*) with ponderosa pine (*Pinus ponderosa*), California black oak (*Quercus kelloggii*), and Douglas-fir (*Pseudotsuga menziesii*) as frequent co-dominants. Regional prairies and savannas support large numbers of plant and animal species. This includes over 750 native plant species of which more than 375 are found principally or exclusively in grassland habitats (Ed Alverson, The Nature Conservancy, unpublished data). Over 95 native vertebrate species are associated with Willamette Valley grasslands, although most do not depend on them exclusively [11]. One of the greatest sources of PNW grassland biodiversity prior to Euro-American settlement was likely to have been invertebrates. Wilson [12] estimated over 1100 species of arthropods were found in upland prairies. This would have included 350-400 species of native bees in oak savannas, many of which were specialized to one plant species or genus. As many as 80% now are likely extirpated or extremely rare (Andy Moldenke, Oregon State University, unpublished data).

Estimates of remaining Willamette Valley native grasslands vary from 2-10%, and almost all are highly degraded [13, 14]. At the time of model parameterization there were only small areas of conserved grassland within the study area, and no compiled map of them. Our study area map of extant vegetation projected that native grasslands covered 6.1% of the study area, or 11% of its historical area (Table S1.2). To set the landscape's baseline 30% conservation target, we adjusted the area of historical study area grasslands to account for the current area that was realistically "out of reach" of future restoration because of conversion to urban uses and high-value agricultural crops. We used the projected area of current prairie and the baseline conservation target to set the key parameters for the grassland scarcity metric.

Table S1.2. Historical versus current native grassland in the study area.

Vegetation type	Est. 1851	Projected Current	Current/1851
Oak savanna	25.2%	3.2%	0.13
Upland prairie	21.6%	2.7%	0.12
Wetland Prairie	10.2%	0.3%	0.04
Total	57.0%	6.1%	0.11

For assessments of future native grassland, we included managed prairie, oak savanna and pine savanna, and managed open oak woodland. Thus, only areas managed for grassland conservation were included in the metric. Because we had no compiled map of conserved grasslands to use in the map of initial vegetation, this meant that the scarcity metric assumed no conserved grassland at run initiation. We excluded IDUs with dwelling units from scarcity metric calculations since the presence of human infrastructure and domestic animals can compromise conservation values. Pine savanna was relatively rare in the initial landscape but emerged as an important potential vegetation type in our projections of future vegetation. We included managed oak woodland because it has emerged as a regional conservation target [9] although not generally prioritized as highly as oak savanna. In our modeling system, oak woodland played an important role for integrated biodiversity conservation and fire hazard reduction. Although it has greater tree canopy cover than savanna (26-40% v. 5-25%), it still can support a strong component of grassland graminoids and forbs, and has high value for many wildlife species [11]. We classified it as a grassland because it was defined by an open canopy with space between tree crowns, a strong grass and forb component in the understory, and only moderate shrub cover.

Envision scarcity metrics are set on a scale of -3 to +3 where 0 means that agents implement policies without additional feedback from landscape scarcities to modify policy adoption rates. Because our landowner survey was used to assess and calibrate agent propensities to restore oak habitats based on current landscape conditions, we therefore set 0 on the scarcity model to the current proportion of restorable grassland area in native grassland (0.11). The scarcity metric rises rapidly when the grassland total drops below 10% of historical levels and reaches a maximum value of 3 at 4%. The metric drops gradually as grasslands increase above 12% of historic levels, and begin to drop rapidly at around 20%, reaching -2 at the 30% target value and then a minimum of -3 at 34% of historic savanna and upland prairie (Figure S1.4).

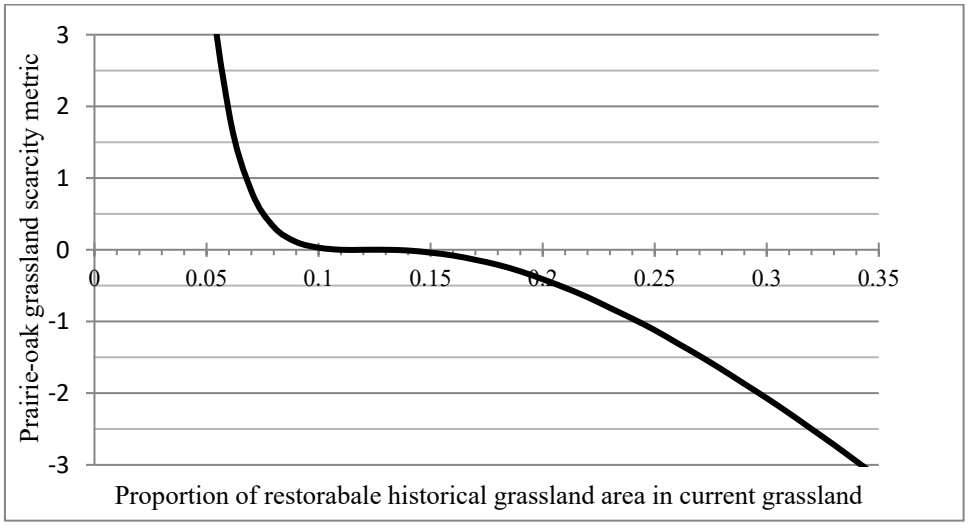

Figure S1.4. Scarcity model for upland native grassland. The scarcity metric varies from -3 to +3, and represents a measure against which the societal goal of preventing scarcities of native grasslands is evaluated. Values > 0 increase agent propensities to restore native grasslands. Values < 0 decrease agent propensities to restore native grasslands.

To achieve these desired relationships the model used a sigmoidal function defined by:

y =(((x-a)/b)^3)/(x*(x*c)) with values of a = 0.12, b = 0.25, and c = 2

where *a* is the point at which y = 0, *b* is a shape parameter that identifies the distance from a to the positive and negative inflection points, and *c* is a parameter that controls the lower limit of y as x increases.

4. Vegetation Succession Submodel

4.1 Overview

The *vegetation succession submodel* is implemented through a plug-in to Envision, the Climate-Sensitive Vegetation State-and-Transition Simulation Model (CV-STSM) [15]. Changes in vegetation occur via two types of pathways: disturbance-driven transitions due to actions by agents (e.g. thinning) or events (e.g. wildfire), and incremental changes due to vegetation succession (e.g., tree regeneration, tree growth and mortality, changes in dominant species). Successional changes in tree size, species composition and stand structure are simulated with probabilistic transitions among different states. Successional pathways for each vegetation state were derived using the Forest Vegetation Simulator (FVS) [16] in conjunction with spatially downscaled outputs of projected future conditions from MC1, a dynamic global vegetation model (DGVM) [17, 18]. Because successional changes occur probabilistically, two IDU's with identical vegetation states can follow substantially different trajectories over time. In concert with these projections of natural succession over time, Envision includes detailed mechanisms for assigning the effects of each management treatment to each vegetation class, as well as successional trajectories constrained by management goals (e.g. oak savanna restoration maintains savanna tree composition and structure as trees grow, and sustains a grassland ground layer that determines surface fuels). If management is not renewed, fuels and vegetation type transition back to unmanaged conditions on a time scale specified for each treatment type.

Vegetation dynamics were implemented using extensive vegetation data, modeled outputs, and expert opinion. Each vegetation type has a suite of attributes that determine potential successional pathways, fuel loadings and structure, and management outcomes. Succession, management, fire, and development interact in space and time through a variety of direct and indirect pathways. For example, lack of management can allow fuels accumulation, thereby facilitating a high-severity fire, which can simultaneously initiate a new vegetation type and delay future development, and through this alter both successional trajectories and future management. Climate influences succession through changes to transition pathways and probabilities due to altered site productivity and the emergence of new potential vegetation types (PVTs) [15] that could establish following a high-severity fire.

Each successional state includes four characteristics used to model succession, management, and wildfire (dominant/subdominant tree species, quadratic mean stem diameter (QMD), canopy closure, canopy layering), as well as five fuel characteristics required for the wildfire modeling that also can be changed by management (surface fuel model, canopy cover, canopy height, canopy base height and canopy bulk density [19]. We used a large set of regional, plot-level tree lists to parameterize each state and simulate transitions under each process, while including vegetation types from further south to bracket warmer climates. Within-state variability in the tree lists led to variable, probabilistic outcomes for each process. For example,

the presence of trees larger than the QMD in some stands meant that both thinning treatments and fire could change the dominant tree species and/or increase the QMD. Simulated best management practices (BMPs) for thinning (including density thinning and savanna or woodland restoration) targeted smaller trees for removal and/or preferentially retained desired species, while mixed-severity fire caused greater mortality to smaller trees and/or less fire-resistant species. Divergent outcomes for treatment and fire could thus arise from a single initial vegetation state (Figure S1.5). (Additional details in Supplement S2.)

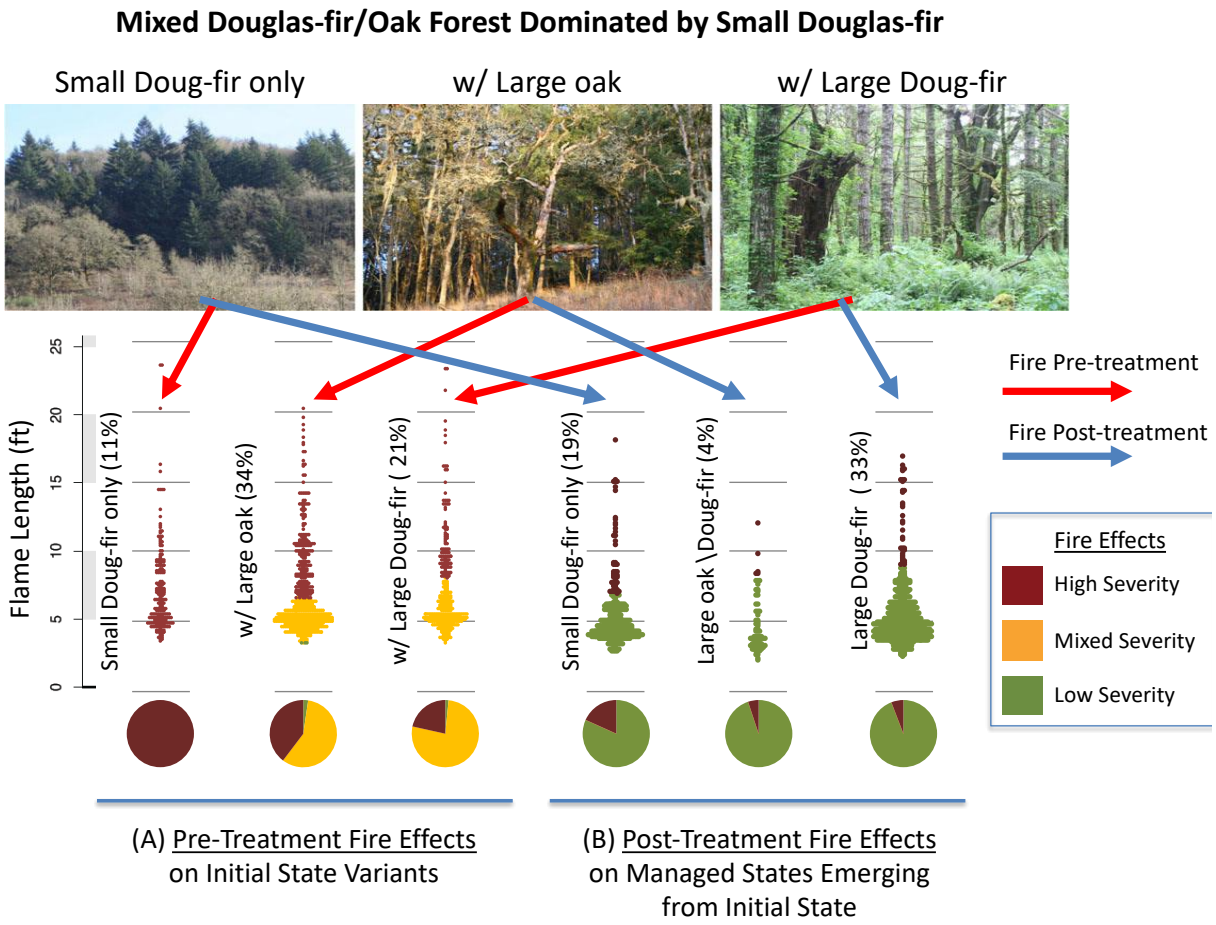

Figure S1.5. Probabilistic transitions allow variable management and fire outcomes for a single vegetation state. Based on empirical tree lists, the presence of low-density, large trees can vary within a vegetation state, leading to different outcomes for thinning or fire. (A) Pre-treatment fire effects on variants of a mixed Douglas-fir/oak forest dominated by small Douglas-fir. (B) Post-treatment fire effects on each variant following density thinning with surface fuels reduction. Percentages show frequency of each fire or management variant based on regional tree-list data. Flame length thresholds and violin plots show relative numbers of outcomes for each variant at 97th percentile fire conditions. Pie charts (bottom) summarize percentages for each fire severity class.

4.2 Submodel Design

The vegetation succession submodel alters detailed vegetation types under the influence of spatially explicit annual climate drivers derived from the same GCMs that drive the fire

model. Current vegetation types were characterized using local and regional data sources, including uncommon types that have become regional conservation priorities. We identified future potential vegetation types (PVTs) for selected GCMs using the DGVM MC1. For PVTs not represented by extant local cover types, we selected appropriate regional cover types as models. Representatives for these new cover types were selected from those found in the nearest areas currently occupied by those PVTs, and with dominant tree species already present in the study area, as the most likely new forest types to emerge within the 50-year simulation timelines.

Based on MC1 simulations, these new cover types were only allowed to establish following a stand-replacing fire. Stand regeneration following a high-severity fire depended on the presence or absence of sprouting tree species and the climatically determined PVT. New cover types could emerge post-fire only when the current PVT did not support the pre-fire cover type in the burned IDU, and when the dominant trees species were present in the burned IDU or an adjacent IDUs to provide local propagules. If the PVT changed again to a different one that did not support this cover type before saplings could become established, the stand changed to a grass-forb stage of a cover type supported by the current PVT.

The specific effects of annual climate drivers on succession was simulated based on extensive testing using outputs from MC1, which identified changes in site productivity as the best predictor of changes in tree growth rates. We translated changes in MC1 productivity to Douglas-fir site index values (SI) (Supplement S2: Sect. 5-6) so that we could crosswalk between MC1 and the Forest Vegetation Simulator (FVS) [16]. FVS simulations were applied to replicate sets of regional plot-level trees lists for each cover type and vegetation state (see below) under a wide array of SI values so that probabilistic transitions could be calculated for any vegetation state in any location under any projected climatic conditions. Within-state variability in the tree lists led to variable (one-to-many), probabilistic outcomes for each transition.

The plant growth conditions used to simulate transitions in a given location at a given time thus were determined by the joint influence of physical (e.g., soils) and climatic conditions present in that location during that time step. Transitions were further constrained by the projected PVTs for that location in that time step. Transitions for managed states were developed using FVS in the same fashion as for unmanaged succession but transitions were constrained to follow the intended management outcome (e.g., a successional transition from oak savanna to oak-fir woodland was not allowed under the oak savanna management regime).

To incorporate within-state variation for management and fire disturbances beyond what was needed to model succession, we derived two types of state variants from FVS simulations applied to the replicate tree lists for each vegetation state. Structural variants specified whether and how the dominant tree species or dominant diameter class could be altered by thin-from-below treatments due to the presence (or absence) of trees larger than the QMD. In a similar fashion, fire-effects variants identified how mixed-severity fires could change the dominant tree species or dominant diameter class due to mortality of smaller trees and/or less fire-resistant species. The proportion of each variant in a state, derived from FVS simulations using the tree lists, determined the transition probabilities for that state under a selected management treatment or a mixed-severity fire. For example, the presence of trees larger than the QMD in some stands meant that both thinning treatments and fire had potential to change the dominant tree species and/or increase the QMD. Thinning BMPs frequently targeted smaller trees for removal and or

preferentially retained desired species; mixed-severity fires caused greater mortality to smaller trees and/or less fire-resistant species. Because of this, divergent outcomes for treatment and fire could arise from a single initial vegetation state.

The coupled succession-management-fire system thus supports a diversity of possible outcomes and interactions among the three processes. The combination of structural variants and related fire-effects variants in unmanaged stands, and the variety of available treatment types, resulted in a rich array of possible fire behavior from initially similar stands. The modular structure of the state and transition systems thus generated a large range of potential behaviors from relatively parsimonious initial state assignments.

4.3 Submodel Parameterization

We used a set of 2,092 regional, plot-level tree lists to parameterize transitions for each process (i.e., management, succession and fire) and the couplings among processes (Supplement S2: Sect. 3-4). The set included plots and vegetation types from southern Oregon and eastern Oregon to bracket warmer climates represented by the projected MC1 future PVTs. Replicates of each vegetation state we used to incorporate within-state variability in probabilistic transitions. For each process, we applied FVS with a newly revised version of the Pacific Northwest variant [20] to the replicate set of each state to determine all possible transitions and their probabilities.

The full suite of CV-STSM land cover types included 12 basic successional cover types with 118 discrete, successional vegetation states (~½ unmanaged and ½ managed), and 38 land use/land cover categories, primarily agricultural and urban (Supplement S2: Sect. 1-2). Four of the successional cover types represent forest types not currently found in the study area but projected as potential vegetation types (PVTs) under MC1. They were represented by cover types with dominant tree species that currently occur in the study area but not as dominants (Figure S1.6).

Based on FVS simulations, the original set of 58 unmanaged successional states generated 354 possible successional transitions (one size larger QMD, a cover type transition, or both) under each set of plant growth conditions (SI x PVT). The addition of the 60 managed states generated ~850 possible successional transitions at a given SI and PVT. When crossed with all possible combinations of PVT and SI, this led to total of 36,654 possible successional transitions. For management, crossing the 58 unmanaged successional states with the 9 treatment types led to a total of 1,349 possible management transitions and a total of 1,898 when renewal treatments were included. For fire, the inclusion of all agricultural and developed states (some unburnable), the unmanaged successional states (with fire-effects variants as well as augmented fuels states), and the managed successional states (with surface fuels variants), produced a total of 480 unique fuels states.

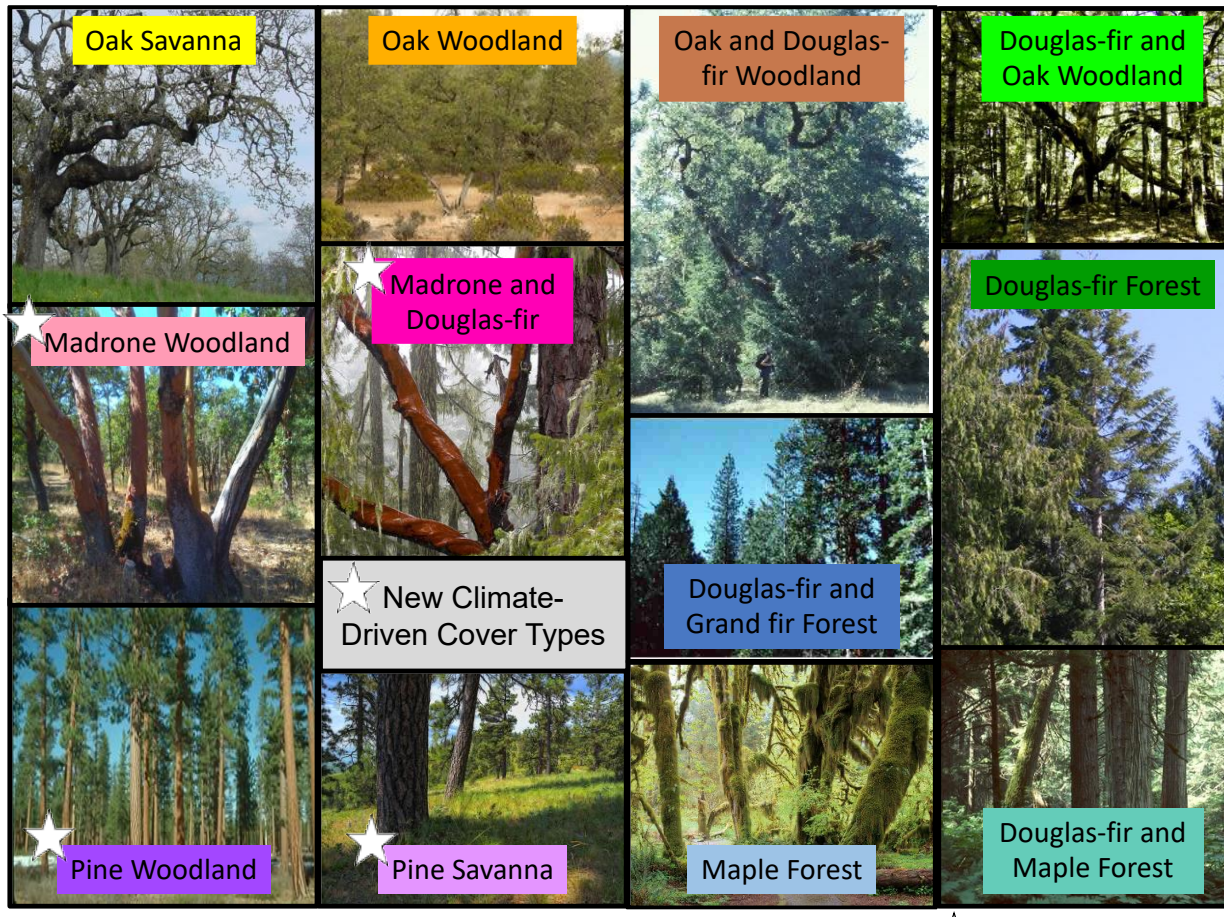

Figure S1.6. The twelve successional cover types parameterized for the STSM. ☆ indicates novel cover types projected under climate change.

5. Wildfire Disturbance Submodel

5.1 Overview

Our goal was to develop a process-based fire modeling system with spatially and temporally explicit ignitions and fire spread that a) were sensitive to local context and landscape change, b) followed a probabilistic, long-tailed size distribution characteristic of wildfire regimes, c) were sensitive to variability in fire-weather, and trends in climate, and d) could be tracked over the course of individual simulation runs to assess the roles of past decisions and stochastic events.

Wildfire behavior is simulated using the minimum travel time algorithm (MTT) to model fire spread and severity [21], which has been applied extensively in wildfire decision-support systems used for fire management (e.g., FlamMap [19]) and research [22-24]. The wildfire submodel executes fire prediction and ignition submodels each year using a dynamically updated information exchange between Envision's polygon-based system and the FB-API grid system to pass landscape conditions to the wildfire submodel, simulate individual fires at the selected ignition locations, and return results to Envision to update the vegetation and fuels states of each

IDU that burns as well as interpret fire impacts for risk-production models.

For each simulated fire, the FB-API requires specification of an ignition location, burn period, fire weather, and fuel moistures linked to a spatially defined landscape with fuels characteristics and topography. A core innovation of the model was that we relied on empirical relationships between daily ERC, fire probability and fire size to link simulated fires to daily fire weather and ignition probabilities generated using climate change drivers. For readers unfamiliar with the fire literature, the Energy Release Component (ERC) is a proxy for the available energy (BTU) per unit area (square foot) within the flaming front at the head of a fire. It is a function of the fuel model and live and dead fuel moistures based on the past seven day's weather. Fuel model G is widely used for assessing fire danger because it contains all size classes of dead fuels and both herbaceous and woody live fuels. Daily variations in ERC are due to changes in moisture content of the various fuels present, both live and dead. Due to its composite fuel moisture structure, the ERC is considered a relatively stable evaluation tool for wildfire modeling.

As described in sections below, a key feature of the wildfire submodel is that three sources of stochastic variability were incorporated to mimic wildfire's uncertainties. First, the replicate daily "fire lists" for each climate scenario allowed multiple representations of future fire weather from a single daily climate data stream. Second, fires that ignited during a model run were selected by applying a pseudorandom number generator to the daily ignition probabilities, thereby generating different sets of simulated fires from the same fire list. Finally, probabilistic controls on ignition location added further variability.

The user, however, can control wildfire variability in several ways. First, Envision allows the user to specify that a constant seed is used for the random number generator at the start of an Envision session. Employing a constant seed enables users to select an identical set of fires for a series of model runs. Combined with the use of pseudorandom number generators for other probabilistic Envision mechanisms (e.g., agent decisions and vegetation succession), this ensures that a specified series of simulation runs can be reproduced with identical outcomes in a new Envision session. At the same time, it also allows users to generate comparative model runs of different management or development scenarios under same climate scenario with identical sets of fires. Although the same fires are selected, because ignition locations depend upon dynamic attributes such as population density, they may ignite in different locations. For this reason, several further features were built into the fire model to allow users to run simulations with full stochastic variability of fires; to create more controlled contrasts between model runs of different scenarios; to input manually modified fire lists to test specific hypotheses; or to use an identical set of fires located in identical locations for multiple model runs.

To implement the wildfire submodel in Envision and couple it with other SES submodels required building and integrating seven primary components. We next introduce of each component, and then detail its design and parameterization in sections below: 1) establishing regional fire-climate relationships; 2) dynamic projection of ignition locations and occurrence; 3) simulating climate impacts on future fire weather; 4) fuels assignment and fire effects calibration; 5) fire model execution; and 6) final calibration through validation to study area fire history.

The submodel applies a fire prediction system to estimate daily wildfire probabilities and

sizes under different weather conditions (Sect. 5.2.1). Estimates were based on empirical relationships between energy release component (ERC), and historical ignition numbers and associated fire sizes [22] from a large assessment area extending beyond the study area's current climate envelope. Similarly, fuel moisture data were assigned using empirical relationships between ERC and fuel moisture from Remote Automatic Weather Stations (RAWS) data. Daily wind speeds and azimuths were assigned using local RAWS and weather data. Our work preceded [25]who refined and adapted the methods described here. Their paper provides additional methodological details.

Ignition locations were assigned using a dynamic spatial probability model developed from historical fire occurrence in the Willamette Valley [26] (Sect. 5.2.2). The model incorporated distance to major and minor roads, as well as local human population density, the latter changing over time. A predictor of how ignition numbers increase with population growth, similar to that of Syphard et al. (2007), was implemented to adjust ignition numbers annually.

To simulate climate change, we derived daily fire weather from regionally downscaled climate streams using selected General Circulation Models (GCMs) and emissions scenarios, and calibrated these to the study area using empirical and modeled ERCs for the historical period (Sect. 5.2.3). The statistical models and procedures described above were incorporated in an R module (R Core Team) (2010) and executed prior to Envision simulations to generate 20 replicate "fire list" files for the historical period (1985-2006) and the future (2007-2099) under different GCMs. Each list comprises probabilistic daily fire weather parameters (ERC, wind speed and azimuth), an ignition probability, a burn period, and fuel moistures for each day of each year.

We assigned initial surface fuel models and canopy fuels to each successional state and burnable agricultural state using a variety of data sources, fuels references, and modeling tools (Sect. 5.2.4). An iterative procedure was used to jointly calibrate fuels data, flame-length thresholds for tree mortality, and fire effects under different fire weather conditions. This initial calibration was used for an online survey of regional fire managers (Supplement S3). We adjusted fuels data and flame-length thresholds to achieve fire severity targets recommended by a plurality of fire managers for selected vegetation states, and extrapolated results to other vegetation states. Each vegetation state had up to three flame length thresholds that determined whether a burned IDU experienced a low-severity, mixed-severity, or high-severity fire. Fires that did not change the vegetation state were classified as low severity. Fire that caused sufficient tree mortality to change the vegetation state but did not top-kill all trees were classified as mixed-severity. Fires that top-killed all trees, returning an IDU to a grass-forb state, were classified as high severity.

Once all fire-related model components had been implemented and parameterized individually, they were coupled in Envision using a wildfire submodel execution sequence (Section 5.2.5) for extensive testing to validate and calibrate system behavior. Final calibration was achieved by iteratively producing 25 replicates Envision runs for the historical period and adjusting ignition probabilities and burn period for different fire size-classes until modeled fire-size distribution, number of fires, total area burned, and maximum fire size closely approximated those of the fire record (Sect. 5.2.6).

5.2 Submodel Component Design and Parameterization

5.2.1 Establishing Regional Fire-Climate Relationships

5.2.1.1 Model design

Historical fire and weather data were obtained from an assessment area ~50 times that of the study area, extending 120 km north and 225 km south to capture ERC-fire relationships in the warmer climate forecast for the study area over the next century. Four representative Remote Automatic Weather Stations (RAWS) were selected within the wildfire assessment area and each historical fire was assigned to the closest station. We developed logistic regression models between ERC and fire occurrence [27], and ERC and fire size. The predicted fire size from the logistic regression model was converted to a burn period since the MTT algorithm simulates fires by duration rather than size. A statistical relationship between fire size and expected burn period was determined by simulating 10,000 random ignitions over a range of burn periods and using the outputs to build a translation equation between fire size and burn period. We used similar data and procedures to establish regional relationships between ERC and fuel moistures, and to model local wind speeds and azimuths by time of year.

5.2.1.2 Wildfire assessment area

A wildfire assessment area was established in ArcGIS and all recorded fires [28] (dates recorded: 8/5/1988-11/30/2008; 4,216 ignitions) occurring within this boundary were used for analyzing relationships between energy release component (ERC) and historical wildfires. The 38,800 km^2 area was bounded on the north by the north-south midpoint of the Willamette Valley (near the city of Salem, Oregon) and on the south by the Oregon/California border. Fires to the north of the boundary were considered to have occurred in a region of greater fire suppression capability (closer to the city of Portland and with higher human population density than the study area). The southern boundary was intended to capture hotter climatic conditions than the study area currently experiences, but within the range that would be expected under future climate in the next 50-100 years, while still being largely comprised of vegetation types similar to that of the current and anticipated future vegetation of the study area. The western boundary of the wildfire assessment area followed the Coast Range crest, while the eastern boundary approximately followed a contour line that divides the older Western Cascades from the newer High Cascades, which contains substantially different vegetation. The difference in annual average maximum temperatures between the Eugene WSO Airport, OR (Period of Record: 12/1/1939 to 3/31/2013) near the study area and the Medford WSO AP, OR (Period of Record: 1/1/1928 to 3/31/2013) near the southern end of the fire assessment area was 2.2° C, and the difference for the peak fire season (July 15 –Sept. 30) was 4.1° C (source: Western Regional Climate Center, wrcc@dri.edu, accessed 3/5/2014). This compares with an average predicted warming of a multi-model ensemble of atmosphere–ocean general circulation models (AOGCMs) of 3.1 C by the 2080s in the PNW [29].

Four geographic zones expected to experience different fire conditions were established in the wildfire assessment area based on three longitudinal divisions: the southern Willamette Valley, the Umpqua Valley, the higher elevations dividing the Umpqua and Rogue River drainage basins, and areas that include both lower and higher elevations in and around the Rogue

and Illinois River Valleys. Each of these areas includes valley floors up into higher elevations. Four Remote Automated Weather Stations (RAWS), one from each zone were selected for modeling the relationship between historical values of daily ERC, wildfire size and number of wildfires. Latitudinal dividing lines were used to assign each historical fire to one of four RAWS stations for analysis (Table S1.3, Figure S1.7). Although each zone contains substantially different elevations, our assignment of RAWS to large areas of varying topographic conditions is consistent with (and even more fine-tuned than) similar uses of a single RAWS stations to assess ERC over large areas [22, 30]. Comparison of the fire regimes in terms of fire frequencies and fire sizes within the Willamette study area in relation to the larger fire assessment area showed that the two areas experience similar levels of fire exposure.

Table S1.3. Wildfire Assessment Zones and associated remote automated weather stations (RAWS).

Zone*	Station	Elev. (m)	Latitude	Longitude
1) South Willamette Valley	Village Creek, OR	457	44 15 09	-123 27 50
2) Umpqua Valley	Mt. Yoncalla, OR	610	43 38 20	-123 19 33
3) Umpqua and Rogue River Valleys divide	Silver Butte, OR	1211	42 51 32	-123 22 42
4) Rogue River and Illinois River Valleys	Provolt Seed Orchard, OR	360	42 17 23	-123 13 49

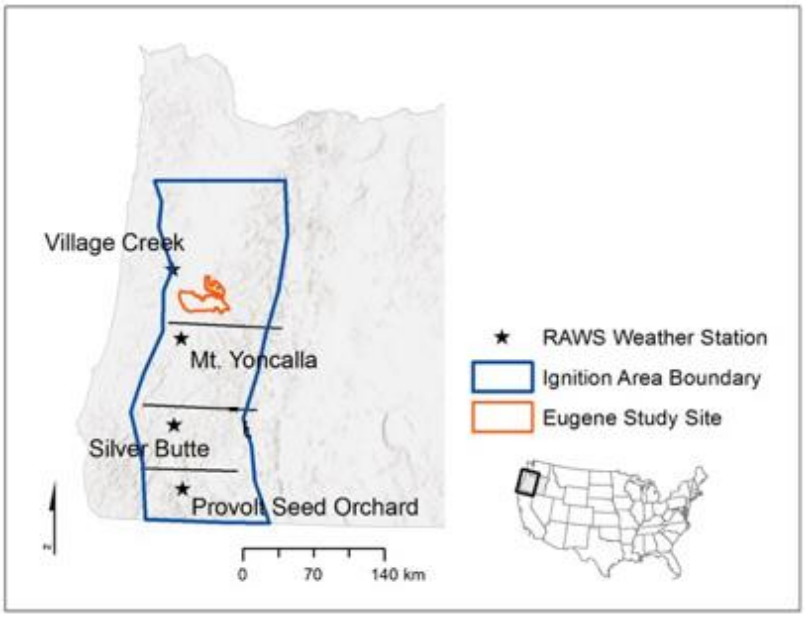

Figure S1.7. Wildfire assessment area zones and RAWS. The 38,800 km^2 area was divided into four zones, each associated with a RAWS to assign the climatic conditions of each fire. UTM northings of the zone divides (latitude in deg/min/sec) from north to south were:

Northern Boundary - UTM Latitude: 4982950 m N (45 04 00)
Zone 1-2 Divide - UTM Latitude: 4845958 m N (43 46 00)
Zone 2-3 Divide - UTM Latitude: 4766367 m N (43 03 00)
Zone 3-4 Divide - UTM Latitude: 4708994 m N (42 32 00)
Southern Boundary – UTM Latitude 4649776 m N (42 00 00)

5.2.1.3 Statistical models for fire probability and fire size

Statistical relationships between ERC and fire were built for both fire probability and fire size. Data for the historical relationship between ERC and fire occurrence in each wildfire assessment zone (Figure S1.8) were used in conjunction with the frequency of each daily ERC to estimate fire probability on a given day using logistic regression in R. For some GCMs, MC1 projects future ERC values that exceed those of the historical records in the wildfire assessment area, and fire probabilities were assumed to increase according to the relationship derived within the bounds of empirical data. Data for the relationship between fire size and ERC (Figure S1.9) were used to estimate a distribution of fire sizes for a given ERC using logistic regression. The distribution of fires sizes at a given ERC was assumed to follow a negative exponential function.

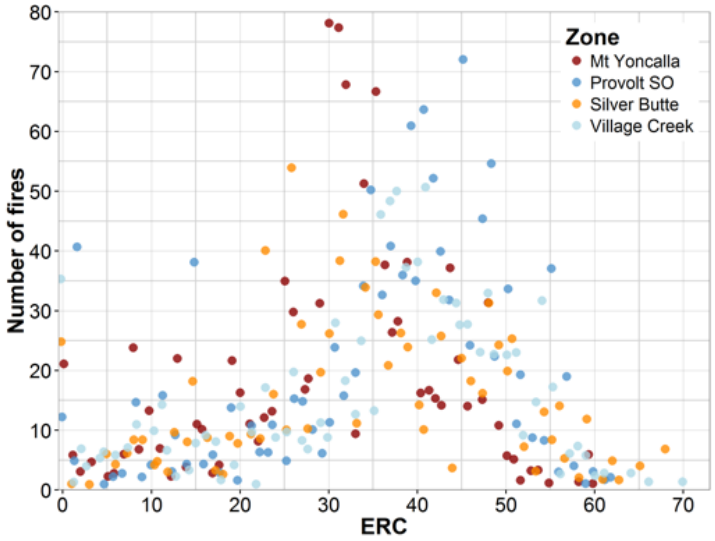

Figure S1.8. ERC versus number of fires for the wildfire assessment zones used to build relationships between ERC and daily fire probability.

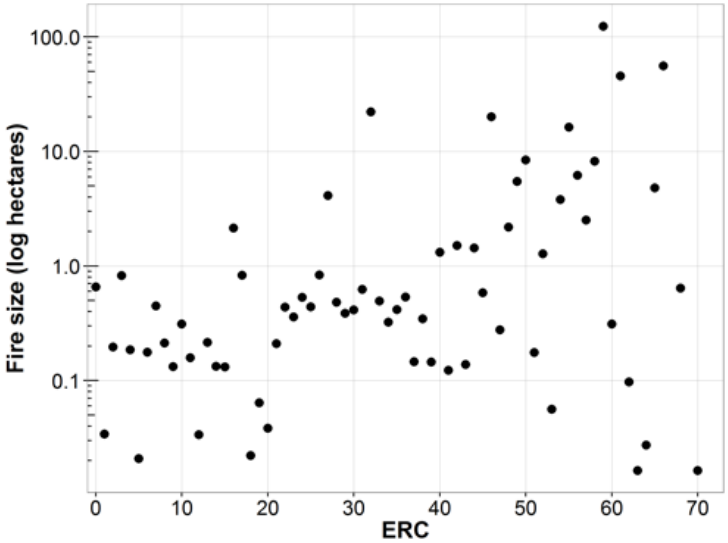

Figure S1.9. Relationship between average fire size and ERC from historical data within the wildfire assessment area. A negative exponential distribution of fire sizes was assumed at each ERC and used to predict fire size for the wildfire submodel.

Because the MTT fire spread algorithm uses inputs of time rather than fire size [21] to obtain the fire size predicted by the fire prediction system it was necessary to translate expected fire size (ha) to burn period (minutes). We created a fire-size burn period distribution with Flammap by simulating multiple sets of 100 random ignition points with burn periods ranging from 30 min to 8000 min. Wind speed, azimuth and ERC were fixed at 18 mph, 220 degrees and ERC 60, respectively. The simulated fire sizes and corresponding burn periods were used to estimate a second-order polynomial linear regression model using fire size as predictor and burn period as dependent variable (Figure S1.10). This relationship was then used to calculate a burn period for each fire that generated on average the predicted fire size according to the relationship between fire size and ERC.

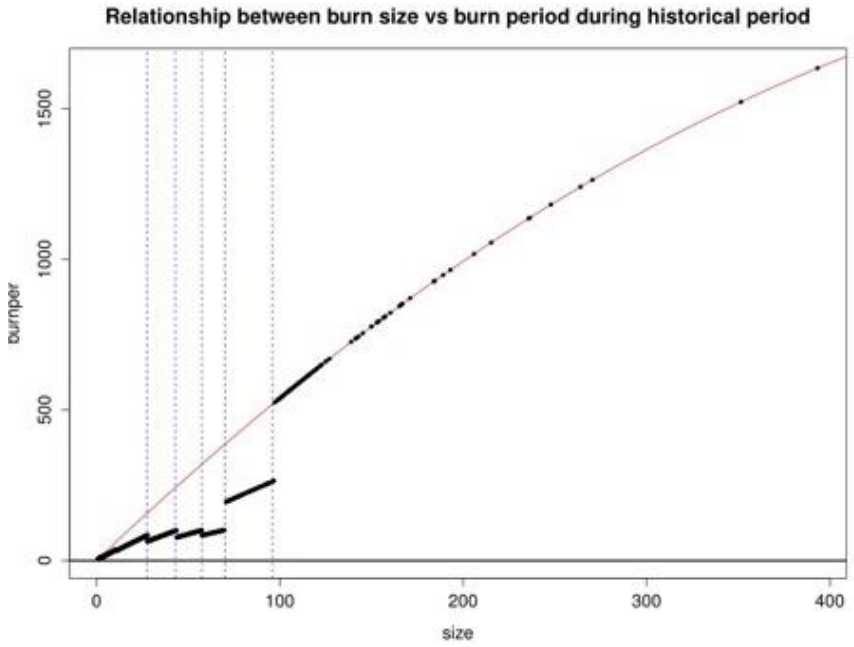

Figure S1.10. Relationship between fire size and burn period developed from fire simulations with Flammap.

5.2.1.4 Fuel moistures

Fuel moisture data required for FlamMap were assigned using empirical relationships between ERC and fuel moistures reported in the historical RAWS data. Fuel moistures were calibrated and assigned as a function of ERC using the same data set generated for the statistical relationships between ERC, fire probability and fire size with the addition of one further RAWS (Oak Knoll station in northern California). The latter RAWS included ERCs higher than those found in the Wildfire Assessment Area and closer to the extreme values projected under the Hadley GCM. Because fuel moisture tends to reach a low-value asymptote at high ERC values, we set a maximum ERC above which we assigned a constant set of lowest fuel moisture values.

Because the Willamette Valley Ecoregion's Mediterranean climate (Köppen climate class Csb, Kottek, Grieser [31]), with warm, dry summers and cool, wet winters is projected to continue under climate change, the modeled fluctuation of herbaceous fuel moistures with ERC was adjusted to mimic the seasonal dynamics of herbaceous species senescence with summer drought and green-up with the initiation of fall rains. This involved the use of dynamic fuel

models (Scott & Burgan 2005), as well as constraints on moisture fluctuation in herbaceous fuels during the rainy season. These assumptions meant that herbaceous fuels tended to slow spread rates and reduce flame lengths during the off-peak season when they largely remain green, and to increase spread rate and flame lengths during the peak fire season when they are almost completely senesced.

To mimic the seasonal dynamics of herbaceous fuels senescence and green-up we constrained the seasonal fluctuations of herbaceous fuel moistures during the rainy season. Throughout the rainy season (typically October-June), grasses and herbaceous fuels are green and retain high moistures even on hot days. Only after herbaceous vegetation senesces in the summer drought do these fuels cure and dry, allowing their moisture to quickly equilibrate with outside humidity. For these reasons, we used dynamic fuel loading functions to allow the transfer of live herbaceous fuels to the dead fuel load during peak fire season. During the off-peak season, fuel moistures were constrained so that they did not drop below the thresholds that transferred live herbaceous fuels to the dead category. Custom fuels with both live and dead herbaceous components allowed the dead fine fuels to equilibrate with humidity, but held the live herbaceous fuels in an uncured state. Specifically, live herbaceous fuels were assumed to be uncured until the typical peak fire season (July 15-Sept 30). Outside peak fire season, herbaceous fuel moistures changed with ERC but were not allowed to drop below a threshold of 75% moisture, at which point 50% was transferred to the dead herbaceous load while retaining the bulk density of the live herbaceous fuels. During peak fire season, herbaceous fuel moistures were assumed to follow the ERC-derived relationships in successional vegetation and non-irrigated pastures. When herbaceous fuel moistures were <=30%, all herbaceous fuels were transferred to the dead fuel load. Fuel models for grazed pasture, hay and grass seed were further constrained to relatively high moistures regardless of ERC or time of year to prevent excessive fire size under in these agricultural types, which are also likely to be quickly suppressed by landowners with fire suppression equipment. An intermediate approach was applied to unmanaged grasslands that include high levels of dead thatch (e.g., remnant prairie, abandoned pasture). Dead fine fuels were allowed to fluctuate with ERC, while live herbaceous fuels were held to high fuel moistures until the peak fire season at which point they were considered cured.

5.2.1.5 Wind speed and direction

Winds were modeled independently from fire probabilities based on local RAWS data from 2000-2010. Wind speed and direction data were summarized to create a monthly distribution of values for each variable from April through November. We used a single distribution for the remaining months. We then sampled from the distributions to assign a wind speed and azimuth for each day. We used a gust factor adjustment for the wind speed (Crosby and Chandler 1966) to account for measurement bias in the RAWS weather station.

5.2.2 Dynamic Ignition Locations and Occurrence

5.2.2.1 Model design

The probabilistic identification of ignition locations each year, including dynamic updates of their numbers and distribution in response to landscape and human population changes was critical to coupling SES processes in Envision. The Willamette Valley ignition

location model of Sheehan [26] produced an ignition probability surface based on logistic regression of historical ignitions. Following incorporation into Envision, the ignition model was modified for other factors expected to influence future ignitions such as the effect of human population growth on ignition numbers.

5.2.2.2 Ignition locations

Extensive statistical analysis of historical Willamette Valley ignition locations yielded spatial probability surfaces for both human and lightning ignitions [26]. Because the Envision study area is located on the lower-elevation valley floor and foothills, it is dominated by human ignitions, and for this reason the human ignitions model was used in Envision. The final model incorporated variables for the distances to major roads (highways, arterials, and collectors), and minor paved roads (minor collectors and local roads) as well as human population density within the surrounding 2.6 km^2 (1 mi^2). An IDU's distance to road does not change during an Envision run, whereas its population density was dynamic and updated each annual time step. Therefore, at each time step, the ignition model first generated an updated ignition probability grid and then selected an ignition location for each fire using Monte Carlo methods.

5.2.2.3 Ignition numbers

Population density is dynamic in Envision, and because of this, the parameterization of ignition probabilities from Sheehan's [26] spatial analysis of historical fire locations can lead to localized increases in ignition probabilities due to nearby population growth in simulations of the future. Because the sum of probabilities in the PDF must total one in any given year, an adjustment to overall fire probabilities was necessary to prevent increases in population density in some locations from reducing ignition probabilities in others. The effect of population density on ignition probability, however, was three orders of magnitude less than the effect of distance to roads and thus accounted for no more than a 2% increase in fire probabilities over a 50-year model run, despite much larger increases in a population density.

The effects of spatial variation in local population density on ignition probability is not, however, a sound basis for projecting temporal changes in ignition numbers due to regional population growth. To assess the effects of regional population growth on the number of ignitions in the Willamette Valley Ecoregion, a spatial database of fires in Oregon from 1960-2005 from the Oregon Department of Forestry [32] was combined with Oregon population growth data [33] and analyzed using multiple linear regression.

The ODF database includes all reported fires statewide that resulted in response from a fire protection agency. The latitude and longitude of each fire is recorded along with the date, fire size, and numerous descriptive variables, including detailed categorization of how each fire started. Using ArcGIS [34], the wildfire data was clipped to the Willamette Valley Level III Ecoregion (WVE) [35]. The WVE includes the valley floor and foothills and is the broader geographic area from which the project's study area was selected. Fire counts were summed by year. Fire data prior to 1967 were discarded due to potential underreporting during the initial years of data collection. To control for the potential effects of fire weather on the number of wildfires in a given year, the average burning index (BI) of all fires was computed for each year. BI is a measure of how fast a fire could spread and how hot it could burn, and a function of the Energy Release Component (ERC). In this way, both the confounding effects of variation in fire

weather severity, as well as that of potential trends in fire weather over time were taken into account in the analysis. Data values for BI of N/A (not applicable), NN (none noted), and missing data all appeared to indicate that burning index was assessed to be 0 or insignificant. Different approaches that ranged from treating all such instances as missing data, or treating all such values as 0 were tested and had only small influences on model parameter values. However, treating all instances of missing data as a value of 0 produced the lowest p values and highest parameter estimates for both for BI and population growth in regression model as well as the highest r^2 values, and was used for final calibrations.

The Willamette Valley contains 70% of Oregon's human population and is the key driver of Oregon's population growth. Because population growth records are broken down by county and city, but not by geographic areas such as the Willamette Valley, Oregon's annual population growth from 1960-2005 was used as a surrogate for Willamette Valley population growth. Both the annual fire count and population growth were relativized to 1967 values so that proportional changes in population could be regressed against proportional changes in number of fires.

A multiple linear regression model of proportional changes in yearly fire count as a function of proportional changes in population growth and burning index (to control for fire weather, e.g., ERC) was developed using SAS [36] as follows. Residuals were assessed for normality and no data transformations were required. Two extreme outlier years of high and low numbers of fire (1970 and 1981) were excluded from analysis. With these exclusions, a total of 3012 fires were used to calculate the annual totals for the 37 years of data used in the analysis.

The results showed a strong effect of both population growth and annual fire weather on changes in the number of fires (Eq. 1).

Eq. 1. $FIRE = -1.6647 + 0.97950 * POP + 0.02199 * BI$

$F(2,34) = 15.24, p<0.0001, R^2 = 0.47$

Where FIRE = annual proportional change in number of fires in the WVE; POP = annual proportional change in Willamette Valley population; BI = average burning index of all reported fires in a given year

The effect of population growth was strengthened rather than diminished when fire weather was controlled for (Eq. 2), indicating that trends in fire weather were not responsible for the increase in the number of fires during this period. Adjusted r^2 dropped from 0.44 to 0.21, population growth effect size decreased substantially, and overall model significance decreased.

Eq. 2. $FIRE = -0.09088 + 0.72574 * POP$

$F(1,35) = 10.32, p<0.0028, R^2 = 0.23$

When fires < 1 acre (0.405 ha) were removed from database to test the effects of including only fires that spread substantially from their source, explanatory power of the model was reduced slightly and population growth effect size increased slightly (Eq. 3).

Eq. 3. $FIRE = -1.32221 + 1.00532 * POP + 0.01771 * BI$

$F(2,34) = 11.68, p<0.0001, R^2 = 0.41$

The equation derived from this analysis resulted in a 0.97% increase in ignitions for every 1% increase in human population – nearly a doubling of ignitions for a doubling of population.

The only study we were aware of to quantify the relationship between population growth and numbers of ignitions in conditions comparable to those of our study area was Syphard et al. [1]. They examined California wildfires and determined that the number of fires reached a maximum at intermediate population densities as a consequence of a) an increase in ignitions with greater numbers of people and b) a decrease in burnable fuels after some threshold of population density. We compared our results to theirs in terms of population density and effect size. Based on their results (Figure S1.11), doublings of population density in the interval between ~5-25 people/km^2 were correlated with ~80% increases in the number of fires. Based on 2000 census data, the population density of the unincorporated rural areas of the Eugene study area (4721 of the total 11,942 in the study area) was ~5.9 people/km^2. Population projections used for the simulations are that study area populations will increase to 74,550 in the next 50 years. The different population growth scenarios project that the proportion of these new residents that live in incorporated areas (including expanded Eugene-Springfield urban growth boundaries) may vary from a high of 95% under the most compact growth scenario to a low of 65% under the most dispersed growth scenario. This translates into year 50 rural population densities that range from 9.6-32.7 people/km^2. Our calculated rate of increases in ignitions as a function of population growth is thus 21% higher than that found in California by Syphard et al. [1] across a similar range of population densities. Their finding that the rate of increase in fires declined and then became negative as densities reached 40 people/km^2 was attributed to reductions in burnable fuels. In our model, these two factors are distinct, since we model both changes in ignitions due to population growth as well as changes in fuel type and distribution due to population growth and land management.

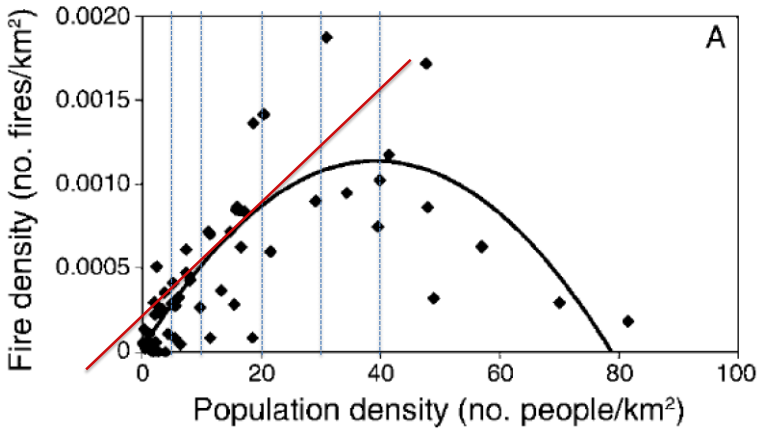

Figure S1.11. Relationship of population increase and number of fires in California. Doublings of population density in the interval between ~5-25 people/km^2 were correlated with ~80% increases in the number of fires. Modified from Figure 6 of Syphard et al. [1].

In Envision, we combined the effects of regional population growth on ignition numbers with those of localized effects on ignition distribution for two reasons. The first is that it appears likely from comparing the results of Sheehan [26] to ODF records that the main driver of

increased ignitions due to regional population growth was the increased use of roads, and increases in activities near them that start fires (e.g. recreational activities such as hiking, camping and fishing). In contrast, increases due to changes in local population density are more likely to be driven by the activities of nearby landowners (e.g., uses of farm machinery, logging activities). This may explain why local population density had such a minor effect on the spatial distribution of ignitions in Sheehan's analysis. To avoid inflating total impacts, we adjusted the 0.97% increase in ignitions for every 1% increase in human population to compensate for the ~0.04%/year increase used to adjust the ignition model for increases in local population density.

5.2.3 Simulating Climate Impacts on Fire Weather

5.2.3.1 Model design

To simulate climate change, we derived daily fire weather based on regionally downscaled climate streams from selected General Circulation Models (GCMs) and emissions scenarios, and calibrated these to the study area. This involved four key steps:

1) Selecting a local RAWS and acquiring daily historical fire weather data, including ERC fuel model G values;
2) Computing monthly ERC fuel model G values (the finest temporal resolution of modeled ERC data) in the area of the local RAWS for selected future climate streams as well the modeled historical period using MC1, a dynamic global vegetation model (Bachelet et al. 2001, Lenihan et al. 2003);
3) Calibrating the modeled monthly average ERCs to the monthly averages of the RAWS ERCs for the common historical period;
4) Probabilistically generating daily future ERCs from the monthly means based on a regression model of historical daily ERCs as a function of monthly mean ERCs.

The resulting process generated daily ERCs for the historical period and the future (2007-2099) under selected GCMs. Once needed modifications and calibrations were completed, the final step was to localize model performance to the study area. Localization was necessary because ignition probabilities and burn periods were calibrated to a larger landscape area with a broad range of topography, vegetation, and suppression capabilities. Finally, the methods and calibrations were used to generate the 20 unique daily "fire lists" comprised of ERC, winds, ignition probabilities, and burn periods for each climate scenario – historical period (1985-2006), MIROC A2 (2007-2099) and Hadley A2 (2007-2099).

5.2.3.2 Model parameterization

To validate whether modeled MC1 ERC values represented those of the study area, we ran MC1 for its historical period (1896-2006) on a single 800-m grid cell that corresponded to the location of a local RAWS. We selected the Village Creek RAWS from among three candidate sites based on its geographic location, elevation and completeness of records (1985-2006). Although there were differences in ERCs among the different RAWS, the general patterns and range of values were similar. Because MC1 produced only monthly average ERC values, we compared these to the RAWS monthly averages. Analysis of the fit between the historical

RAWS and MC1 ERCs showed that MC1 substantially overpredicted ERCs and shifted higher ERCs toward earlier in the year (Figure S1.12 A).

We explored a wide array of data transformations through regression analysis in SAS [36] to derive a model that better calibrated MC1 to the RAWS data (Eq. 4). This equation was reverse engineered to calibrate the MC1 historical ERCs to the RAWS ERCs for modeling, and similarly to calibrate future monthly ERC data streams for the Hadley A2 and MIROC A2 GCMs (Eq. 5).

Eq. 4. sqrt(MC1_ERCG) = 0.49211 + 0.85896 * sqrt(RAWS_ERCG)

F(1,192) = 576.57, p<0.0001, R2 = 0.75

Eq. 5. MC1_ERCG_mod = ((sqrt(MC1_ERCG) -0.49211)/0.85896)^2

The process yielded a stronger fit between MC1 ERCs and study area ERCs (Figure S1.12 B).

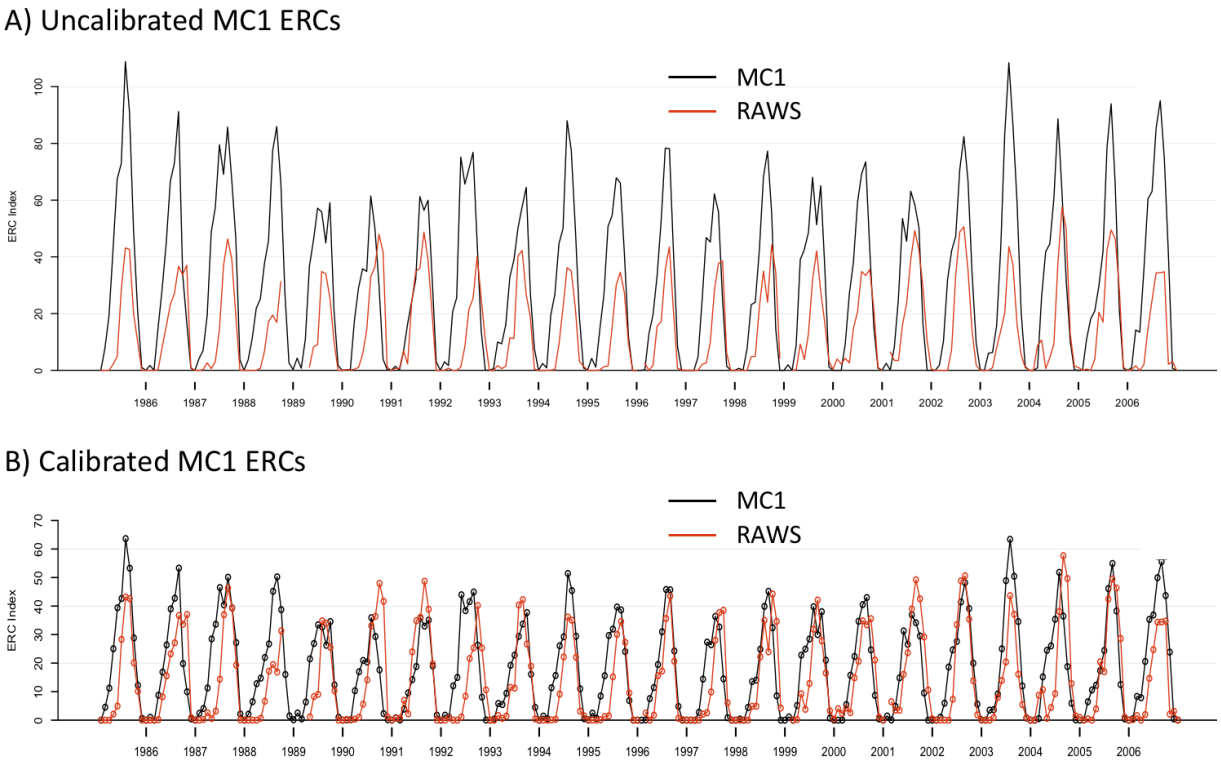

Figure S1.12. Modeled monthly ERC calibration to RAWS records. A) Uncalibrated MC1 monthly ERCs v. RAWS ERCS. B) Calibrated MC1 monthly ERCs v. RAWS ERCS. RAWS data from Village Creek, 1985-2006.

The final step was to generate daily future ERCs from the monthly means based on a regression model of historical daily ERCs as a function of monthly mean ERCs. First, the daily RAWS ERC values were processed to create monthly means and standard deviations. Next, the standard deviations were regressed against the monthly means. Residuals were checked for normality and a log transformation was used to generate the final equation showing how variance increased with greater monthly ERCs (Eq. 6).

Eq. 6. RAWS_ERCG_sd = --1.80293 + 3.22763*log(RAWS_ERCG + 0.1) ;)

$F(1,213) = 199.49$, $p<0.0001$, $R^2 = 0.48$

Finally, we used this equation to generate ERCs for each day of the year for the historical and future climate streams based on the calibrated MC1 monthly values (taking into account leap years). This was achieved using the SAS RANNOR function, which returns a variate that is generated from a normal distribution with mean 0 and variance 1 using the logic of Eq. 7.

Eq. 7. ERCday = ERCmonth + (ERCmonth_sd*rannor(seed))

When Eq. 7 was used to generate daily ERCs, the seed was selected randomly for each fire list. This allowed the monthly MC1 ERC data generated from the single GCM data stream available at the time to support multiple future realizations of daily fire weather. Because no burn periods were greater than one day, serial autocorrelation of daily ERCs was unnecessary. If >24-hour burn periods for multi-day fires had been generated, we were prepared to use a model based on the daily series of historical RAWS ERCS to organize the randomly generated ERCS into autocorrelated daily series.

When the complete set of equations of the fire generator system (Sect. 5.2.1) were invoked to create the daily fire lists, the daily ERCs produced were used to generate the associated daily burn probability, burn period, and fuel moistures.

5.2.4 Fuels Assignment and Fire Effects Calibration

5.2.4.1 Model design

We assigned initial surface fuel models and canopy fuels (canopy cover, canopy height, canopy base height and canopy bulk density) to each successional state as well as to burnable agricultural states using a variety of data sources, fuels references, and modeling tools. These included simulations using the Forest Vegetation Simulator (FVS) with the fire and fuels extension [37] on our 2,000 tree plot lists; fuels data from 239 plots at seven sites in the southern Willamette Valley with mixtures of oak, oak/conifer and conifer habitat (Yospin et al. 2012); Scott and Reinhardt's [38] reference photos and fuel model descriptions; and a GIS overlay of LANDFIRE data (http://www.landfire.gov/) with our fuels assignments.

An iterative procedure then was used to jointly calibrate fuels data, flame length thresholds and fire effects under different fire weather conditions. This began with initial parameterization based on FVS-FFE modeling to establish initial flame length thresholds for state transitions. To further calibrate the relationship between flame length and mortality, we adjusted these results based on a simple set of first principles for expected patterns of fire effects among different stand structures, in conjunction with Nomograms from Reinhardt and Ryan [39] and the FOFEM software [39, 40].

We used this initial calibration as the basis for an online survey of regional fire managers. We used the survey to check their agreement with, or recommended adjustments to, our first principles, and to identify their expectations for fire effects on selected forest stand types under both current 97th percentile fire weather conditions as well as more extreme 97th percentile conditions projected under the Hadley GCM. We invited 17 wildfire managers to participate in

the survey. Invitees were purposively selected from various state and federal agencies for their potential knowledge about wildfire behavior and effects in oaks vegetation types in western Oregon. Ten invitees participated in the survey for a response rate of 59% (see Supplement S3 for the survey and results).

We next adjusted fuels data and flame length thresholds for tree mortality as needed to achieve the expected fire severity targets recommended by a plurality of fire managers for each surveyed vegetation state and its associated species, and extrapolated based on the revised first principles to each other vegetation state. Each state has up to three flame length thresholds that, when an IDU burns, determine whether the result is a low-severity fire, a mixed-severity fire (two potential levels) or a high-severity fire. Operationally, low-severity fires were defined as those that did not cause enough tree mortality to change the vegetation state. They could, however, set back fuels accumulation, and, in a treated IDU, delay the return to an unmanaged successional state and fuels. A mixed-severity fire was defined as one that caused enough tree mortality to change the vegetation state but not to top-kill all trees. Two levels of mixed-severity fire were defined when FVS simulations indicated two such state-changing outcomes for a specific vegetation type were possible. Compared to a mixed-severity I fire, a mixed-severity II fire experienced greater tree mortality, resulting in fewer trees comprised of mostly larger size classes and more fire-resistant species. A high-severity fire was defined as one that top-killed all trees, returning the IDU to a grass-forb state.

We extrapolated survey results to the full set of unmanaged and managed successional states by modifying fuels data and flame length thresholds based on the survey results. These included fire-effects "variants" that identified how the presence of trees larger than the quadratic mean stem diameter (QMD) could changes the dominant tree species or QMD following a fire due to mortality of smaller trees and less fire-resistant species. Finally, we performed extensive comparative tests on all vegetation states and made final adjustments to ensure consistency and compatibility of results with our stated assumptions and the guidance of the fire managers.

5.2.4.2 Model parameterization

The sensitivity of simulated fire severity to interactions between factors such as canopy base height, surface fuel models and flame-length thresholds necessitated extensive calibration to achieve fire managers' recommended outcomes for different ERCs and for peak- and off-peak-season herbaceous fuel moistures. We conducted calibration tests using the Envision-Flammap adapter and the Flammap API. Unmanaged states were simulated from the initial study area landscape to situate different vegetation types in their landscape contexts (e.g., topography). Managed states were created by simulating each management treatment individually across the entire initial landscape to derive large numbers of IDUs in each treated state.

We illustrate the final outcomes of this testing procedure, and the resulting system sensitivity to ERC and season, for two situations: First, we show fire severity under 97th percentile current ERC (56) v. the projected 97th percentile ERC under the Hadley GCM for 2007-57 (78) in unmanaged vegetation types, illustrating the large shifts from low- and mixed-severity fire to high-severity fire under more extreme ERCs with cured herbaceous fuels (Figure S1.13). Second, we show cured v. uncured herbaceous fuels at ERC 56 following density thinning with surface fuels reductions, illustrating the effect of grass and forb phenology on flame length and fire-severity in thinned stands (Figure S1.14).

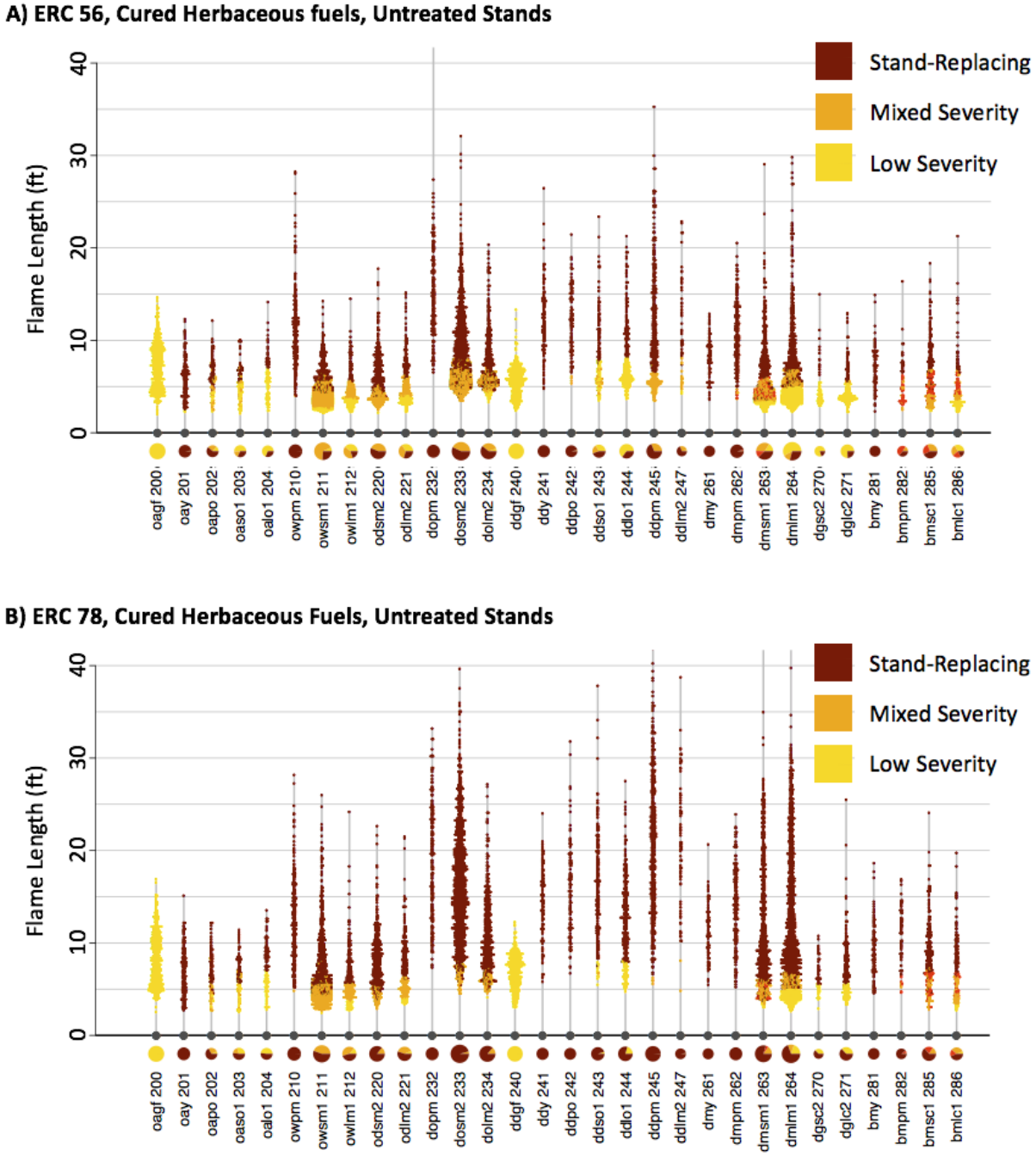

Figure S1.13. Flame lengths and fire severity at ERC 56 and 78 for unmanaged, selected successional vegetation types under peak fire season conditions. Each dot represents the outcome for a 90 m cell from the study area landscape. Pie charts summarize outcomes. Vegetation-type codes and numbers are explained in Supplement 2: Sect. 2.

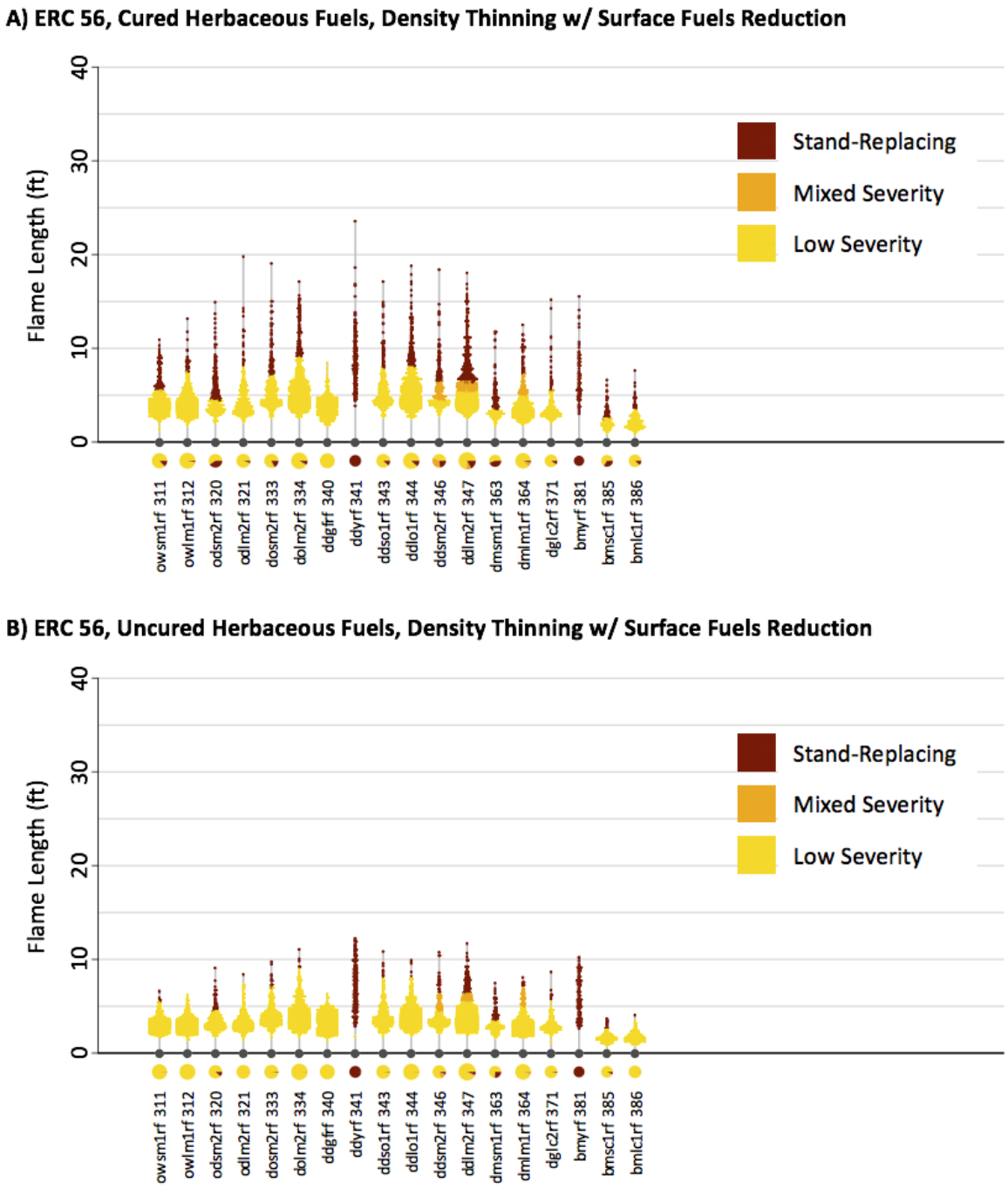

Figure S1.14. Flame lengths and fire severity at ERC 56 during peak and off-peak fire season conditions for selected vegetation types following density thinning. Each dot represents the outcome for a 90 m cell from the study area landscape. Pie charts summarize outcomes. Vegetation-type codes and numbers are explained in Supplement 2: Sect. 2.

5.2.5 Fire Model Execution

At run execution, all available fire lists are read into Envision for potential use. The adapter builds a binary fuels landscape for the FlamMap API to translate the fuels from the polygon-based IDU geometry to a cell-based grid (default grid is 90 x 90 m). To do this, it uses a crosswalk table that identifies the plurality IDU (by area) of each cell so that the IDU's values can be assigned to that cell. The translation process uses a grid-cell template that stores IDU topographic variables, which are invariant throughout the simulations, and contains fields for the required fuels values, which are updated each annual time step. Next, a single fire list is assigned probabilistically for the model run from those available for the associated climate scenario. Each time step, the fuel loadings associated with each IDU's vegetation state are translated from Envision to the cell-based grid. Ignition probabilities in the daily fire list are adjusted for study area population growth and the ignition model is updated for changes to localized population density. The wildfire submodel next applies Monte Carlo techniques to draw a set of fires and associated simulation parameters (fuel moistures, burn period, wind speed and azimuth) for that year. Each selected fire is assigned an ignition location using Monte Carlo methods. The wildfire submodel then simulates each individual fire independently, and the resulting fire perimeter and gridded flame lengths are written to files. The latter file is overlaid with IDU polygons using the crosswalk table to translate results back to the IDU geometry. The average flame length for each affected IDU is calculated from the pixel data and used to interpret fire effects. A fire effects lookup table translates flame lengths to vegetation state changes and disturbance types. The table includes all vegetation states with their five landscape (LCP values) used to simulate fire, and flame length thresholds to assign state changes based on flame lengths. The table is jointly referenced by FlamMap (for LCP values) and Envision (to implement state changes after flame lengths have been returned from FlamMap). To address boundary effects, we used a 36 x 50 km bounding rectangle to simulate fire spread into and out of the study area. Fuels outside the study area were parameterized using LandFire data and were not updated during modeling since they were outside the simulation area. Similarly, the ignition model was not updated outside the study area but stayed constant based on initial values.

A number of user interface options offer control over how the system translates between the polygon-based IDU system and the FlamMap grid. For example, the IDU-to-grid lookup table is computed for 30, 60 and 90 m grids to allow users to choose the resolution of FlamMap simulations. For this study, the default 90-m grid was used. The user may also reset default parameters for the percentage of an IDU that must burn to be recorded as a fire, and the flame length recorded (e.g., the average or maximum flame length of all grid cells). For this study, only IDUs that experienced a fire on more than 50% of their area were recorded in Envision as having burned, and the IDU flame length reported was the average flame length of all grid cells comprising an IDU.

5.2.6 Final Calibration through Validation to Study Area Fire History

Initial tests using the fire model to simulate 25 replicate Envision runs for 1985-2006 revealed too many ignitions and much larger areas burned than recorded in the Oregon Department of Forestry [32] records for the study area. Simulations were run with randomly

selected fire lists on the initial landscape with all agent decisions disabled except for timber harvest, and analyzed as described in Table S1.4. By reviewing the system as a whole, we implemented three core modifications:

1) We tested alternative statistical approaches and data transformations for calibrating the burn period and burn probabilities, and derived more suitable equations for both. When candidate models did equally well under the historical climate, we examined outcomes under the more extreme Hadley GCM. Those with more conservative extrapolations of the effects of ERC on burn period and burn probability outside the bounds of the historical data produced outcomes that were more consistent with other studies of future fire for the region under the Hadley climate [41, 42].
2) Many of the ignitions were from fires occurring under low ERCs that were predicted to be <1 ha in size. Because FlamMap could not simulate fires <0.81 ha (the size of the 90 m cell used), we deleted all such fires from the fire lists. This preventing simulating ignitions that were not predicted to spread substantially from their ignition location.
3) Visual examination of simulated fire maps showed extremely large grassland fires, including pastures, hayfields, grass seed fields and prairies. ODF records did not document the area burned in different fuel types but did list the primary fuels at the ignition point. We used ignition fuels as a proxy to compare the simulated proportion of ignitions in grass fuels v. forest fuels for fires >50 ha to those recorded in the Willamette Valley Ecoregion. Simulations accorded well with the ~25% recorded by ODF, but also showed large, simulated grassland fires burning outside the peak fire season. This led us to implement the procedures that constrained herbaceous fuel moisture fluctuation outside the time of year when herbaceous fuels were expected to be senesced.

With these changes implemented, we performed a final round of calibrations to the study area fire record.

Final calibration to the study area fire regime was achieved by iteratively simulating 25 replicates of the historical period (1985-2006), and adjusting daily burn probabilities and burn periods in the fire lists using SAS [36] each time until selected fire metrics closely approximated those of the ODF fire records. The metrics selected were the number of fires >1 ha, total area burned, maximum fire size and proportions of fires in different fire size-classes. The mapped fire record was clipped in ARCGIS to the study area boundaries to calibrate the number of fires, area burned and maximum fire size. However, fire size-class distributions were calibrated to those of the Willamette Valley Ecoregion with a 10 km buffer (WVE assessment area) to capture a larger area of similar vegetation, topography and fire suppression capabilities with more fires than that of the study area.

We based these metrics on the 22-year totals for the historical period rather than on annual fire occurrence for two reasons. First, the relatively small study area had too few fires on record for meaningful statistical analyses of annual fires. Second and perhaps more importantly, because our simulation system was designed to produce multiple realizations of possible fire regimes from even a single climate stream, it was essential to simulate and calibrate multiple realizations of the historic fire regime from a single realized past.

Because the simulation model generates probabilistic realizations of fire to account for uncertainties of whether fire might occur on a given day and its range of possible behavior,

bracketing the range of future uncertainty required assumptions about where the realized past fell within the range of possible pasts. After extensive testing, we decided that calibration using the median of simulated study area fire metrics, and the average size class distribution of the entire ecoregion best achieved our goals. First, it ensured that simulations of the recent past would be equally divided into those that had more fire and those that had less fire than the actual past. While many local fire managers consider we've been "lucky" to escape disaster, this seemed the most defensible assumption. Second, it created the potential for fires as large as those experienced in similar landscape conditions in the ecoregion as a whole to occur in some alternative realizations of the past. Alternatively, using the average of the simulated study area metrics constrained results so that the largest fires never approached the size of the largest in the WVE assessment area but instead were constrained to sizes almost identical to those of the historical record. The iterative steps of the calibration process are shown in Table S1.4.

Table S1.4. Calibrating and adjusting fire lists to historical fire record.

A) Calibrations for the historical period. B) Applying calibrations to future climates.

A) Calibrate fire lists for the historical period

1) Prepare metrics from the ODF historical record (1985-2006)
    a. Compute the number of fires >1 ha, total area burned, and maximum fire size for the study area.
    b. Classify all recorded fires for the WVE assessment area into 9 fire-size percentile bins and compute the average fire size in each bin. The bins were set up to primarily discriminate large fires (largest to smallest size classes: top 1%, 1-2%, 2-3%, 3-5%, 5-10%, 10-30%, 30-50%, 50-75%, 75-100%).
2) Prepare historical fire lists
    a. Compile all 20 historical fire lists for 1985-2006 into a single database.
    b. Delete all fires predicted to be <1 ha.
    c. Apply ignition probability adjustment for population growth (Sect. 2.3.4) to historical period fire lists based on regional population growth projections. Adjustments were set so that the middle year of the simulation period received no adjustment. This weighted ignitions toward more recent years without changing overall probabilities.
3) Conduct simulations and assess outcomes
    a. Perform an Envision session with 25 simulation runs of the historical period (1985-2006) using randomly selected fire lists. Compile all output lists of simulated fires, retaining the run numbers.
    b. Produce comparative metrics for each Envision run and compute medians and averages for selected metrics.
    c. Compare Envision fires to ODF records for the selected metrics.
4) Apply adjustments to fire lists as needed.
    a. Adjust burn probabilities.

i. Multiply all burn probabilities by a constant value calculated as the (number of study area fires >1 ha in the ODF record)/(median number of fires >1 ha for the 25 simulation runs). This adjusts the median number of expected simulation fires to the historical record without changing fire size distribution.

b. Adjust burn periods

i. Use the equation relating ERC to burn period to proportionally adjust the expected fire sizes in each percentile bin toward those of the ODF records. The burn period is produced by the equation:

Eq. 8 $bp = b_0 + b_1X + b_2X^2$

where bi are coefficients of the 2nd order polynomial equation for burn period as a function of predicted fire size, and x is the predicted size of the fire.

To adjust burn period for each bin, we applied the equation:

E. 9 $bp\_adj = b_0 + b_1(X*R_i) + b_2(X*R_i)^2$

to each fire by percentile bin, where R_i = (ODF average fire size)/(Envision average fire size) for the $_i$th percentile bin.

5) Repeat steps 3-5 until desired values are achieved.

6) Once the historical period calibration was complete, the results were applied to the Hadley and MIROC fire lists as follows.

B) Adjust future-climate fire lists based on calibrations to historical period

1) Prepare future fire lists. The 20 fire lists for each future climate scenario were prepared as in A2, except that population growth adjustments to burn probabilities were made so as to align adjustments to the final year of the historical period.

2) Adjust burn probabilities of all fire lists by the proportional adjustment used to obtain the appropriate number of historical fires.

3) Adjust burn periods by percentile bins using the R_i derived from the historical calibration in the burn period equation. However, for the future fire lists, the procedure was modified to assign fires to the percentile bins using the fire-size limits of the historical bins. That is if the lower and upper limits of bin1 were k < predicted fire size <= j, then all future fires with k < predicted fire size <= j would be put into bin1. This allowed shifts in the simulated proportions of fires in each size class due to changes in climate or fuels.

Initial model calibrations required two iterations of adjustments. The final round, which followed the core model improvements, required only one round of adjustments. Results are shown in Table S1.5. Prior to calibration, all simulated study area medians exceeded the ODF record and fire sizes in all but the largest and smallest percentile bins exceeded those of the WVE assessment area. The largest fire size class averaged smaller fires than those of the WVE assessment area but still were much larger than any experienced in the study area. As such, they were not adjusted during the initial calibration given the overall challenges of downscaling fire sizes. Following this calibration, median fire sizes were deemed close enough to study area metrics that no further adjustments were attempted. Although simulated fires in the upper two percentile bins were substantially smaller than those in the WVE assessment area, they were still larger than those experienced in the study area, and the largest fires approached those of the

WVE assessment area. For example, the largest fire in 25 historical simulation runs was 1767 ha, compared to the largest recorded fire of 47 ha in the study area and 2009 ha in the WVE assessment area.

Table S1.5. Comparison of 1985-2006 simulation runs with ODF 1985-2006 fire records pre- and post-calibration.

A) ODF fire record v. simulation medians after and before calibration.

	Total fires >1 ha	Area burned (ha)	Max. fire size (ha)
ODF (n=1)	26	174	47
Envision (n=25) post-calibr.	25	194	59
Envision (n=25) pre-calibr.	38	720	255

B) Average fire sizes by percentile bin

	Average fire size (ha)			Ratio ODF/Envision	
Percentile bin	ODF WVE	Envision post-calibr.	Envision pre-calibr.	Post-calibr.	Pre-calibr.
0-1%	2008	531	1522	3.8	1.3
1-2%	149	79	306	1.9	0.5
2-3%	43	46	171	0.9	0.3
3-5%	31	29	101	1.1	0.3
5-10%	22	16	53	1.3	0.4
10-30%	7.5	6.7	14	1.1	0.5
30-50%	2.5	3.6	4.2	0.7	0.6
50-75%	1.7	2.4	2.6	0.7	0.6
75-100%	1.2	0.8	1.0	1.6	1.2

6. Fire-Decisions-Succession Execution Sequence

The Envision execution sequence uses timers that track the time (annual time steps) in management and/or since cessation of management, and the time since last disturbance (management or fire) to integrate and reconcile changes caused by succession, management, and fire. These timers determine when treated IDUs are available for retreatment, or, in the absence of treatment, the timelines for gradual return to an unmanaged successional state, and for how fuels accumulate or are reset by disturbance (Table S1.6). For example, If an agent ceases management, treatment effects degrade on a specified timeline, and fuels parameters are assigned intermediate values to those of the managed and unmanaged fuels for that cover type and diameter class. If management has not been renewed by the next designated time threshold, the IDU returns to an unmanaged state and successional trajectory. To simulate surface fuels accumulations on unmanaged forests and woodlands, we assigned a 20% increase in fuel loadings after 20 years without management through a set of "augmented" fuel models for each

state. Timelines for fuels accumulation and return to unmanaged states varied by treatment type based on stakeholder guidance.

Table S1.6. Execution sequence for a single time step to determine succession and fuels accumulation in relation to management and disturbance. Annual timers: TSD = time since disturbance, TIM = time in management, TSA = time since cessation (abandonment) of management (renamed TSM = time since last management in paper body). DISTURB >0 = occurrence of a disturbance. MANAGE (10-19) = type of management applied (e.g. density thinning = 14, oak savanna = 10-11). VARIANT = fuels variant, including high quality v. structural restoration, and recently managed v. degraded fuels treatments moving back toward an unmanaged state.

Timing	Action	Logic	Affect Cols	Process

Pre-Actor	Reset DISTURB	If (DISTURB > 0)
		{TSD=0 and
		DISTURB = -DISTURB}
		Else
		TSD=TSD+1
		FLAMELEN=0
			DISTURB, TSD	SWCNH-Pre

	Set Flame lengths	FLAMLEN=length	FLAMLEN	FlamMapAP
	Set Fire-related Disturbances	DISTURB=disturbance code based on vegcalls_fire_vddt_transitions.csv VEGCLASS=code based on current VEGCLASS, VARIANT, and vegclass_fire_vddt_transitions.csv VARIANT = 1 for all fires	DISTURB VEGCLASS VARIANT	FlameLen Disturb Handler
Actor Decision-making (Policies applied at this step) MANAGE, ABANDON, …				
Post-Actor	Set Time in Active Management (TIM)	If (MANAGE=0) // unmanaged {If (TIM > 0) TIM=0} Else // in a managed state {If (TSA > 0) TIM=0 Else TIM=TIM+1}	TIM	SWCNH-Post

	Set Time Since Abandonment;
	Reset to -1 if idu is in active management
	Reset TIM to zero is just abandoned
		If (TSA >= 0 and MANAGE>0 and TIM > 0)
		{TSA=-1}
		Else // not in active management
		{If (TSA = 0) TIM=0 // just abandoned?
		If (TSA >= 0) TSA=TSA+1 }
			TSA, TIM	SWCNH-Post

	Check Time Since Abandonment	If (MANAGE = 10) VARIANT=1
		If (MANAGE = 11) VARIANT=2
		If (MANAGE = 12) VARIANT=1
		If (MANAGE = 13) VARIANT=2
		If (MANAGE = 14) VARIANT=4
		If (TSA >= lower threshold) VARIANT=3
		Manage = 10, change to variant 3 at 14 years TSA
		Manage = 11, change to variant 3 at 12 years TSA
		Manage = 12, change to variant 3 at 8 years TSA
		Manage = 13, change to variant 3 at 12 years TSA
			VEGCLASS, VARIANT, MANAGE	ProbVegTrans

		Manage = 14, change to variant 5 at 5 years TSA Manage = 15, change to variant 3 at 12 years TSA Manage = 16, change to variant 3 at 12 years TSA Manage = 17, change to variant 3 at 8 years TSA Manage = 18, change to variant 3 at 12 years TSA Manage = 19, change to variant 3 at 8 years TSA If (TSA > upper threshold) {MANAGE=0 VEGCLASS = VEGCLASS – 100} Manage = 10, 14 years TSA Manage = 11, 20 years TSA Manage = 12, 16 years TSA Manage = 13, 20 years TSA Manage = 14, 10 years TSA Manage = 15, 20 years TSA Manage = 16, 20 years TSA Manage = 17, 16 years TSA Manage = 18, 20 years TSA Manage = 19, 12 years TSA		

	Do Veg Transitions	If(DISTURB <= 0 and MANAGE=0)
		VARIANT (probabilistic)
		
		If(DISTURB = 1)
		VARIANT = 1
		
		If(DISTURB is not fire disturbance)
		Thinning Disturbance (probabilistic)
		Restoration Disturbance (probabilistic)
		Harvest Disturbance (probabilistic)
		
		If (DISTURB <=0)
		Successional transition (probabilistic)
			VEGCLASS, VARIANT, MANAGE	ProbVegTrans

Literature Cited

1. Syphard, A.D., et al., *Human influence on California fire regimes.* Ecological Applications, 2007. **17**(5): p. 1388-1402.
2. Hulse, D., et al., *Anticipating surprise: Using agent-based alternative futures simulation modeling to identify and map surprising fires in the Willamette Valley, Oregon USA.* Landscape and Urban Planning, 2016. **156**: p. 26-43.
3. Nielsen-Pincus, M., R.G. Ribe, and B.R. Johnson, *Spatially and socially segmenting private landowner motivations, properties, and management: A typology for the wildland urban interface.* Landscape and Urban Planning, 2015. **137**(0): p. 1-12.
4. Nielsen-Pincus, M., R.G. Ribe, and B.R. Johnson, *The sociology of landowner interest in restoring fire-adapted, biodiverse habitats in the wildland-urban interface of Oregon's Willamette Valley Ecoregion.* , in *Proceedings of the second conference on the Human Dimensions of Wildland Fire*, S.M. McCaffrey and C.L. Fisher, Editors. 2011, USDA Forest Service, Northern Research Station: Newtown Square, PA. p. 58-66.
5. Garmon, J.R., *Restoring oak savanna to Oregon's Willamette Valley : using alternative futures to guide land management decisions*. 2006: Thesis (M.S.)--University of Oregon,2006.
6. Ulrich, N.D., *Restoring oak habitats in the Southern Willamette Valley, Oregon: A multi-objective tradeoffs analysis for landowners and managers*. 2011, University of Oregon.
7. Pfeifer-Meister, L., et al., Unpublished Data.
8. Pfeifer-Meister, L., et al., *Dominance of native grasses leads to community convergence in wetland restoration.* Plant Ecology, 2012. **213**(4): p. 637-647.
9. ODFW, *Oregon Conservation Strategy*. 2016, Oregon Department of Fish and Wildlife: Salem, Oregon USA.
10. Christy, J.A. and E.R. Alverson, *Historical Vegetation of the Willamette Valley, Oregon, circa 1850.* Northwest Science, 2011. **85**(2): p. 93-107.
11. Vesely, D.G. and D.K. Rosenberg, *Wildlife conservation in the Willamette Valley's remnant prairie and oak habitats: A research synthesis*. 2010, Oregon Wildlife Institute: Corvallis, Oregon, USA. p. 131.
12. Wilson, M.V., *Wetland prairie: contributed chapter, Part I the U.S. Fish and Wildlife Service Willamette Basin Recovery Plan*. 1998, U.S. Fish and Wildlife Service: Portland, Oregon, USA.
13. Hulse, D.W., S.V. Gregory, and J.P. Baker, *Willamette River Basin Trajectories of Environmental and Ecological Change: A Planning Atlas*. 2002, Corvallis, OR: Oregon State University Press.
14. WVOPC, *Strategic Action Plan*. 2020, https://willamettepartnership.org/wp-content/uploads/2020/03/WV-Oak-and-Prairie-Cooperative-SAP-FINAL-3_2020-web.pdf: Willamette Valley Oak and Prairie Cooperative.
15. Yospin, G.I., et al., *A new model to simulate climate-change impacts on forest succession for local land management.* Ecological Applications, 2015. **25**(1): p. 226-242.
16. Crookston, N.L. and G.E. Dixon, *The forest vegetation simulator: A reivew of its structure, content, and applications.* Computer and Electronics in Agriculture, 2005. **49**: p. 60-80.
17. Bachelet, D., et al., *Climate change effects on vegetation distribution and carbon budget in the United States.* Ecosystems, 2001. **4**(3): p. 164-185.

18. Lenihan, J.M., et al., *Climate change effects on vegetation distribution, carbon, and fire in California.* Ecological Applications, 2003. **13**(6): p. 1667-1681.
19. Finney, M.A. *An overview of FlamMap fire modeling capabilities*. in *Fuels Management-How to Measure Success. Proceedings RMRS-P-41*. 2006. Fort Collins, CO: USDA Forest Service, Rocky Mountain Research Station.
20. Gould, P.J., C.A. Harrington, and W.D. Devine, *Growth of Oregon White Oak (Quercus garryana).* Northwest Science, 2011. **85**(2): p. 159-171.
21. Finney, M.A., *Fire growth using minimum travel time methods.* Canadian Journal of Forest Research, 2002. **32**(8): p. 1420-1424.
22. Finney, M.A., et al., *A simulation of probabilistic wildfire risk components for the continental United States.* Stochastic Environmental Research and Risk Assessment, 2011. **25**: p. 973–1000.
23. Ager, A.A., N.M. Vaillant, and M.A. Finney *Integrating fire behavior models and geospatial analysis for wildland fire risk assessment and fuel management planning*. Journal of Combustion, 2011. **572452**, 19 DOI: 10.1155/2011/572452.
24. Andrews, P.L. *BehavePlus fire modeling system: past, present, and future*. in *Proceedings of 7th Symposium on Fire and Forest Meteorology*. 2007. Bar Harbor, Maine: American Meteorological Society.
25. Ager, A.A., et al., *Analyzing fine-scale spatiotemporal drivers of wildfire in a forest landscape model.* Ecological Modelling, 2018. **384**: p. 87-102.
26. Sheehan, T.J., *Modeling Wildfire and Ignitions for Climate Change and Alternative Land Management Scenarios in the Willamette Valley, Oregon*. 2011, University of Oregon.
27. Preisler, H.K., et al., *Probability based models for estimation of wildfire risk.* International Journal of Wildland Fire, 2004. **13**(2): p. 133-142.
28. Short, K.C., *Spatial wildfire occurrence data for the United States, 1992-2011 [FPA_FOD_20130422]*. 2013, USDA Forest Service, Rocky Mountain Research Station.
29. Mote, P.W. and E.P. Salathe, *Future climate in the Pacific Northwest.* Climatic Change, 2010. **102**(1-2): p. 29-50.
30. Ager, A.A., et al., *Network analysis of wildfire transmission and implications for risk governance.* Plos One, 2017. **12**(3): p. 28.
31. Kottek, M., et al., *World Map of the Köppen-Geiger climate classification updated.* Meteorologische Zeitschrift, 2006. **15**(3): p. 259-263.
32. ODF, *Fire Database: Oregon Department of Forestry commonly requested GIS data sets, protection districts [Data file]*. 2010, Oregon Department of Forestry: http://www.oregon.gov/ODF/GIS/gisdata.shtml
33. PSU, *Census Data for Oregon*. 2010, Portland State University: Portland, OR USA, http://www.pdx.edu/prc/census-2010-data-for-oregon.
34. Esri, *ArcGIS Desktop*. 2009, Environmental Systems Research Institute: Redlands, CA USA.
35. PNW-ERC. 1999, Oregon State University, Pacific Northwest Ecosystem Research Consortium: Corvallis, OR USA, http://www.fsl.orst.edu/pnwerc/wrb/access.html.
36. SAS_Institute, *SAS*. 2009, Statistical Analysis Systems Institute Inc.: Cary, NC, USA.
37. FVS, *Forest Vegetation Simulator*. 2010, USDA Forest Service: https://www.fs.fed.us/fvs/.
38. Scott, J.H. and E.D. Reinhardt, *Stereo photo guide for estimating canopy fuel characteristics in conifer stands*. 2005, Fort Collins, CO (2150 Centre Ave., Fort Collins

80526): Fort Collins, CO 2150 Centre Ave., Fort Collins 80526 : U.S. Dept. of Agriculture, Forest Service, Rocky Mountain Research Station.
39. Reinhardt, E. and K.E. Ryan, *How to Estimate Tree Mortality Resulting from Underburning.* Fire Management Notes, 1988. **49**(4): p. 30-36.
40. Reinhardt, E.D., *First Order Fire Effects Model : FOFEM 4.0, user's guide*. 1997, Ogden, Utah : U.S. Dept. of Agriculture, Forest Service, Intermountain Research Station: Ogden, Utah.
41. Rogers, B.M., et al., *Impacts of climate change on fire regimes and carbon stocks of the U.S. Pacific Northwest.* Journal of Geophysical Research-Biogeosciences, 2011. **116**: p. 13.
42. Turner, D.P., D.R. Conklin, and J.P. Bolte, *Projected climate change impacts on forest land cover and land use over the Willamette River Basin, Oregon, USA.* Climatic Change, 2015. **133**(2): p. 335-348.